2025-01-8445

Combustion and Emission Performance from the use of Acid-catalysed Butanol Alcoholysis Derived Advanced Biofuel Blends in a Compression Ignition Engine

S. Wiseman, H. Li, A.S. Tomlin
School of Chemical and Process Engineering, University of Leeds, Leeds, UK, LS2 9JT

Abstract

Low-carbon alternatives to diesel are needed to reduce the carbon intensity of the transport, agriculture, and off-grid power generation sectors, where compression ignition (CI) engines are commonly used. Acid-catalysed alcoholysis produces a potentially tailorable low-carbon advanced biofuel blend comprised of mixtures of an alkyl levulinate, a dialkyl ether, and the starting alcohol. In this study, model mixtures based on products expected from the use of *n*-butanol (butyl-based blends) as a starting alcohol, were blended with diesel and tested in a Yanmar L100V single-cylinder CI engine. Blends were formulated to meet the flash point, density, and kinematic viscosity limits of fuel standards for diesel, the 2022 version of BS 2869 (off-road). No changes to the engine set-up were made, hence testing the biofuel blends for their potential as "drop-in" fuels. Changes in engine performance and emissions were determined for a range of diesel/biofuel blends and compared to a pure diesel baseline. The ratio of butyl-based biofuel components ranged between 65 – 90 vol% *n*-butyl levulinate, 5 – 30 vol% di-*n*-butyl ether, and 5 – 10 vol% *n*-butanol. Formulating the blends to match physical property limits ensured that engine operation was not significantly influenced by changes in these selected properties. Emissions of CO, NO_X, total hydrocarbons (THC), and $PM_{2.5}$ and particle number (PN) size distributions were measured. Compared to the baseline diesel, ignition delays were longer. The brake-specific fuel consumption of some butyl-based blends at high loads was within 5% of the diesel baseline. Most blends caused a less than 3% reduction in peak in-cylinder pressure at high loads, which contributed to maintaining engine efficiency. $PM_{2.5}$ and PN emissions were reduced significantly. CO and THC specific emissions increased relative to diesel for all blends, potentially due to their reduced derived cetane number. This however, resulted in increased premixed combustion favouring reductions in particulate emissions. The competing effects of changes in adiabatic flame temperatures and charge cooling effects, contributed to maintaining blend NO_X emissions close to those of diesel. The results demonstrated the biofuel blends may have the potential to be low-carbon fuels used CI engines.

Key Words: Advanced Biofuels; Engine Performance; Compression Ignition Engine; Ignition Delay; Fuel Consumption; Emissions; Particulate Matter

1. Introduction

Whilst electrification is increasingly being used to decarbonise light-duty vehicles, heavy-duty vehicles, such as those used in agriculture, haulage, and construction, are likely to rely on combustion engines, for the short to medium term [1]. In these sectors, compression ignition (CI) engines fuelled with diesel and other liquid fuels are commonly used. Whilst, in the long term, alternative strategies such as electrification or hydrogen usage may develop for such sectors, the challenges of the high power and energy density requirements of the machinery used in these sectors will need to be addressed. To facilitate rapid decarbonisation, suitable low-carbon alternatives to petroleum-derived diesel are urgently required. Off-grid or backup power generation also still relies heavily on oil-derived fuels for use in generator sets (gensets). These are commonly CI engines fuelled with diesel of different qualities and specifications depending on where they are used. Ultra-low sulphur diesel for example is used for backup power generation in Europe, but in regions such as Sub-Saharan Africa, where gensets could either be the only source of electricity, or could provide back up to solar power within a mini-grid design, the fuel could be of lower quality [2]. In Europe, EN 590 sets the limits for road diesel, and pre-2023, BS 2869 sets the limits for grade II diesel used in off-road applications, including off-grid power generation [3,4]. In America, ASTM D975 sets the standard for diesel [3-5]. Ideally, renewable or low-carbon fuels designed to displace fossil derived fuels for use in existing engines would be 'drop-in' fuels, which meet existing standards and hence would require no modifications to existing engines or infrastructure. One set of potential candidates is advanced biofuels, which are liquid fuels derived from non-food-based feedstocks with a lifecycle reduction in greenhouse gas emissions of at least 50% compared with fossil fuels. Additional benefits of using advanced biofuels are that there would be no increased land use to produce the required feedstocks, resulting in there being no competition with food production. The use of advanced biofuels is mandated in the revised Renewable Energy Directive (RED II), which requires a 3.5% contribution to total energy use in the EU in the transport sector by 2030, due to increase to 5.5% in RED III [6,7].

Advanced biofuels produced from lignocellulosic materials defined in RED II Annex IX can be manufactured using a variety of methods [6]. Acid-catalysed alcoholysis of these feedstocks is a method that produces a tailorable product blend of advanced biofuel candidates [8-13]. The main products are an alkyl levulinate, dialkyl ether, and the alcohol used as the solvent [8-12]. The starting alcohol of interest in this study was *n*-butanol; resulting in butyl (Bu) based blends containing *n*-butyl levulinate (*n*BL, $C_9H_{16}O_3$), di-*n*-butyl ether (DNBE, $C_8H_{18}O$), and *n*-butanol (*n*BuOH, C_4H_9OH). The *n*BuOH derived blends were of interest due to the possibility to meet selected physical property limits and hence to ensure the blends were miscible and stable when the butyl blends were blended with diesel [14].

Studies have shown that blends of these as individual components, or multi-component mixtures, with diesel, have the potential to meet a selection of fuel standard property limits, such as the flash point and kinematic viscosity [14-16]. However, the impact of these fuel blends on the combustion and operational performance of CI engines is variable, with both improvements and detrimental changes relative to diesel found in previous studies [5,11,17-20]. Heat release rates (HRRs), in-cylinder pressures, ignition delays (IDs), brake specific fuel consumption (BSFC), and power output are some of the engine properties that change following the addition of advanced biofuels to diesel [11]. These changes are due to the physical and chemical properties of the fuel blend changing relative to diesel due to the biofuel components being added. Fuel standards have strict limits to ensure that, regardless of the supplier, due to consistent production, there will be safe, efficient, and reliable delivery and storage, and operation of engines. Physical properties with standard limits that influence engine performance include the density at 15 °C, kinematic viscosity at 40 °C (KV40), and derived cetane number (DCN). Additional non-standardised properties that influence engine performance include heat capacity, energy content, and lower heating value (LHV) [5,11,17-20]. These properties will influence the fuel spray and

vaporisation, which impact the BSFC and the ID, and thus the emissions [5,11,18-21].

Table 1. Fuel component properties and standard limits.

Fuel Component	Density at 15 °C (kg/m³)[a]	KV40 (mm²/s)[a]	DCN[b]	Heat Capacity (J/kg K)[c]	LHV (MJ/kg)[e]	Adiabatic Flame Temperature[f] (K)	Enthalpy of Vaporisation[g] (kJ/kg)	Boiling Point (°C)[j]
EN 590 Limits [3]	820 – 845	2.00 – 4.50	>51	None specified	None specified	None specified	None specified	None specified
2022 BS 2869 Limits [4]	>820	2.00 – 5.00	>45	None specified	None specified	None specified	None specified	None specified
Diesel[k]	838	2.813	51	-	42.7	2200 - 2250	250 - 358	160 - 360
*n*BL	973	2.017	14	1962[d]	27.4	2860	325[i]	232
DNBE	768	0.736	100 – 115	2135	38.3	2865	346	142
*n*BuOH	811	2.261	12 - 16	2401	33.1	2450	702	117

[a]measured by an Anton Paar SVM3000, [b]from [22], [c]from [23], [d]from [24], [e]from [5,12,17,25,26], [f]from [27-30], [g]from [23,31-33], [h]at 420 K, [i]at 785 K, [j]from [23], [k]These are typical diesel values.

The properties of the fuel components of interest and the applicable fuel standards' limits are summarised in Table 1. Not all of the biofuel components would meet the physical property limits individually. However, by designing suitable blending strategies it is possible to design 3-component biofuel blends that meet the density and KV40 limits [14]. As shown in the table, DNBE has a significantly higher DCN than typical values for diesel, whereas those for *n*BL and *n*BuOH are lower. Hence, changing the relative fractions of these components would be expected to have a strong influence on the autoignition properties of the blends. The boiling point of each component is likely to influence the effectiveness of fuel delivery from the fuel tank to the cylinder and into the gas phase. High adiabatic flame temperatures could influence thermal nitrogen oxide (NO_X=NO+NO_2) production. High heat capacities and enthalpies of vaporisation would contribute towards charge cooling, reducing in-cylinder temperatures, and therefore are likely to reduce complete combustion and thermal NO_X production. If the changes in these properties result in reductions in emissions whilst maintaining or improving engine performance and fuel consumption, it would make the butyl-based blends potentially attractive advanced biofuel blends to contribute to both RED II and decarbonisation targets [6].

Currently, the addition of oxygenated advanced biofuel components to diesel results in the final fuel being non-compliant with EN 590 or BS 2869, as both of these standards only allow for fatty acid methyl esters to be added as the oxygenated biofuel blend components [3-5]. Therefore, adding the *n*BL, DNBE, or *n*BuOH to the diesel would result in this criterion no longer being met. This however, could unnecessarily add to the challenges of developing advanced biofuel blending components, and it may be that blends containing other types of oxygenated components are able to meet physical property limits within the standards without serious impacts on engine performance. This work therefore aims to investigate the influence of advanced biofuel blending on the combustion, and heat release characteristics of a CI engine.

In addition to decarbonisation targets, engine applications must comply with relevant tailpipe emissions standards. For HDVs the current emissions standard is Euro VI and for non-road mobile machinery (NRMM), such as gensets, the relevant standard is Euro Stage V in the EU [34-36]. For HDVs, the new Euro 7 emissions standard will come into force in the next few years [35,37]. The Euro 7 emissions limits for HDVs are stricter than those of Euro VI [34-36]. For example, the particle number (PN) limit will reduce from 8×10^{11} #/kWh to 6×10^{11} #/kWh for World Harmonised Test Cycles. In addition, there will be a limit introduced for a real driving emissions test of 9×10^{11} #/kWh, with the minimum particle diameter to be included in the PN count to be reduced from 23 nm to 10 nm [34-36]. The reduction in particle size could lead to an increased requirement for more effective exhaust after-treatment systems. However, the use of low-carbon alternative fuels such as oxygenated biofuels that inherently produce lower engine-out emissions could also be potentially useful technologies.

1.1. Review of Combustion and Emissions of *n*BL, DNBE and *n*BuOH Mixtures with Diesel

Blends of DNBE and *n*BL with diesel were studied by Frigo et al. [11] in a Kohler single-cylinder, four-stroke, 441 cm^3 engine. The blends had a fixed DNBE fraction of 4 vol%, with increasing *n*BL fractions of 7, 11, and 13 vol%, and the remainder of the blend being diesel. They found that, with higher *n*BL fractions, the heat release began around 1 CAD later, delaying ignition and reducing the peak in-cylinder pressure by up to 2 bar relative to diesel, because ignition occurred further away from top dead centre (TDC) [11]. IDs were 0.25, 0.40, and 0.55 CAD longer than for diesel for the blends with 7, 11, and 13 vol% *n*BL, respectively. The longer IDs reduced the torque generated at all engine speeds, but at lower engine speeds, the engine efficiency was greater than that of diesel due to the longer IDs allowing for a longer air/fuel mixing time. The indicated mean effective pressure (IMEP) was unchanged, and engine operation was stable for all blends, as the coefficient of variation of the IMEP was below 1% for all the fuels tested [11]. Frigo et al. [11] showed that the addition of butyl-based blends reduced the fuel smoke number (FSN) relative to diesel, but increased CO and total hydrocarbon (THC) emissions, likely due to the longer IDs and reduced in-cylinder pressures [11,12]. Frigo et al. [11] reported small changes in NO_X emissions relative to the diesel baseline for most of the blends tested with both increases and decreases depending on the nBL content. These differences highlight that there is competition between the positive and negative influences of the properties of the different biofuel components shown in Table 1 such as adiabatic flame temperatures, heat capacities and boiling points, which merit further study in order to evaluate their potential as low-carbon alternatives to diesel [3,4,11,27].

Antonetti et al. [12] tested a blend that was representative of the product ratios from alcoholysis using *n*BuOH of *Eucalyptus nitens.* The three-component blend consisted of 70 wt% *n*BuOH, 20 wt% DNBE, and 10 wt% *n*BL, blended into diesel at 10, 20, and 30 vol% and tested in a two-cylinder Lombardini engine. They reported that the engine power did not deviate significantly from the diesel baseline. CO and soot emissions reduced significantly at the different engine speeds tested, with the reductions correlated to the biofuel fraction. However, the NO_X and HC emissions remained consistent with the diesel baseline [12]. These results showed that the utilisation of high fractions of highly oxygenated low-cetane number fuel could improve emissions whilst maintaining engine performance.

Raspolli Galletti et al. [20] tested blends of *n*BL, DNBE, and *n*BuOH with diesel in a two-cylinder, four-stroke Lombardini engine. The two three-component mixtures with fixed 10 wt% *n*BL and DNBE at 60 or 20 %mass and *n*BuOH at 70 or 30 %mass blend respectively, were blended with diesel at 10 and 20 vol% biofuel [20]. They also

tested a biofuel blend of 66.6 %mass *n*BL and 33.3 %mass DNBE. All blends tested produced less engine power due to lower LHVs compared to diesel, and no modifications were made to the fuel delivery system to account for this. The blend of 66.6 %mass *n*BL/33.3 %mass DNBE at 12 vol% in diesel, at 1500 rpm and full load, had a longer ID compared to diesel and a lower peak pressure. However, at 2500 rpm and full load, the ID and peak pressure were similar to those produced using diesel, albeit with reduced engine power [20]. Therefore, the volume of fuel injected and the fuel properties influenced engine performance. Raspolli Galletti et al. [20] reported reductions in CO for the three-component blends but an increase for the two-component blend relative to diesel. NO_X emissions were similar to the diesel for all blends tested. Soot emissions reduced with increasing biofuel blend content, with the 20 vol% blends reducing the particle emissions to around 50% of the diesel baseline [20]. Therefore, tailoring the blend of the three-components could lead to favourable reductions on the soot emissions.

The discussed engine tests did not formulate the blends to meet the different fuel standard physical property limits [5,11,12,17-20]. Creating advanced biofuel fuel blends that comply with the property limits may increase their commercial viability. The work presented here therefore aims to determine and quantify the influence of different butyl-based blends with diesel, on engine performance and emissions, where the blends were formulated to match selected physical property limits in the 2022 version of BS 2869, [4,14].

To achieve the above aim and to determine the influence of the different butyl-based blends, a range of butyl-based blends with diesel that met the property limits were selected [14]. They were tested in a single cylinder engine to determine the influence of the blend composition on the engine emissions and performance parameters typically used to assess the suitability of fuels. The emissions measured included CO, THC, NO_X, PN, and particulate matter. The performance parameters determined included the fuel consumption, ignition delay, heat release rates (HRR), and peak in-cylinder pressures.

2. Experimental Methodology

The formulation of the blends tested in this work was selected by determining blends of *n*BL, DNBE, and *n*BuOH with diesel that complied with the flash point, density, and KV40 limits of 2022 BS 2869, as this is the fuel standard applicable for fuels used in gensets in the UK and Europe [4,14]. The blends were selected based on their physical properties, as well as their miscibility with diesel. These blends were tested on a small engine, under steady-state conditions, at a range of engine loads, to determine the influence of the biofuel blend composition on the combustion and operational performance of the engine. The fuel blending methodology, engine specification, and heat release rate analysis techniques are outlined in the subsequent sub-sections.

2.1. Fuel Blending

The fuel blends tested consisted of the butyl-based three-component blends and an EN 590 compliant ultra-low sulphur diesel (ULSD) containing 7 vol% biodiesel from Crown Oils (UK), referred to as D100. The compositions and properties of the blends are shown in Table 2. LHVs of the blends were calculated using a linear-by-mass blending law based on the values for D100 and each biofuel component [14]. Fuel blends were blended on a volumetric basis and up to 25% biofuel fractions were tested with different vol% of the individual biofuel components. The components used were *n*BL (98%, Fisher), DNBE (99+%, Fisher), and *n*BuOH (99% extra pure, Fisher).

The blend notation is formulated as in the following example: D*X*Bu*X*-75:20:5, where D*X* is the diesel volume percentage, Bu*X* is the biofuel blend volume percentage, and the three subsequent numbers are the volume fractions within the biofuel components in the order of alkyl levulinate (75 %), dialkyl ether (20 %), and then alcohol (5 %).

2.2. Engine Testing Methodology

A constant speed, single-cylinder, EU Stage V emission standard compliant Yanmar L100V engine was used for the engine testing. The engine parameters are summarised in Table 3. The engine was connected to an MG6000 SSY generator (MHM Plant, UK), using an E1C10M H alternator (Linz Electric, Italy), connected to a Hillstone HAC240-10 resistive loadbank through a 230 V 32 A socket. The engine power was calculated using the alternator efficiency at a given generated electrical power. No modifications were made to the engine operation or the fuel delivery system, including keeping the fuel injection timing and pressure constant, as the aim was to establish the potential of these fuel blends as drop-in fuels.

Steady-state engine tests were conducted at the five loads as listed in Table 3 and were run in triplicate for each load. The load settings used (4%, 28%, 50%, 75%, 92%) were similar to those required in ISO 8178 (10%, 25%, 50%, 75%, 100%; constant speed, type D2). Emissions factors were calculated using the ISO 8178 methodology [38]. The steady state tests were conducted to replicate real world use of a genset. The main aim of this testing methodology was to determine the influence of the biofuel blend composition and to compare the performance and emissions to that of diesel.

Table 3. Yanmar L100V engine specification.

Property	Value
Number of Cylinders	1
Cycle	Four-Stroke
Compression Ratio	21.2
Cooling	Air Cooled
Injection	Direct
Injection Timing (CAD before TDC)	13.5
Engine Speed (revolutions per minute (rpm))	3000 ± 100
Maximum Displacement (cm^3)	435
Engine Power (kW)	0.26 – 5.7
Engine Loads Tested (% of max)	4%, 28%, 50%, 75%, 92%

Table 2. Blend compositions tested and their physical properties.

Fuel Blend	Diesel (vol%)	Biofuel (vol%)	*n*BL:DNBE:*n*BuOH (vol%)	Density at 15 °C (kg/m^3)	KV40 (mm^2/s)	LHV[a] (MJ/kg)	DCN[b]
D100	100	0	0	838	2.813	42.5 – 42.9	51
D90Bu10 – 65:30:5†	90	10	65:30:5	846	2.453	41.4	49.8 – 50.3
D90Bu10 – 75:20:5	90	10	75:20:5	845	2.493	41.3	49.0 – 49.3
D90Bu10 – 85:10:5†	90	10	85:10:5	850	2.513	41.1	48.1 – 48.3
D90Bu10 – 85:5:10	90	10	85:5:10	851	2.524	41.1	47.7 – 47.8
D90Bu10 – 90:5:5†	90	10	90:5:5	851	2.516	41.1	47.7 – 47.8
D75Bu25 – 85:10:5†	75	25	85:10:5	866	2.294	38.8	42.7 – 42.1
D75Bu25 – 90:5:5†	75	25	90:5:5	869	2.309	38.7	41.9 – 42.1

† indicates the blends that were used in the HRR analysis. [a]Determined using a linear-by-volume blending law [14]. [b]Determined using a linear-by-mole blending law for the three-component blends, combined with linear-by-volume when blended with diesel.

In-cylinder pressure was measured using an AVL GH14D pressure transducer (19 pC/bar sensitivity) connected to an AVL FlexIFEM charge amplifier. Pressure-volume (PV) and pressure-crank angle (P-CA) traces were generated using an in-house LabVIEW programme and were used to determine the ID. When logging the in-cylinder pressure, data for 100 cycles was captured, enabling engine stability to be determined. IDs in the engine were defined as the difference between the timing of the start of injection and the start of combustion, defined as the maximum dP/dCA after TDC. The fuel tanks were on a balance, with a precision of 10 g, and the mass of fuel used per test was used to determine the BSFC for an individual test. The changes in performance parameters and emissions relative to the D100 baseline are represented using a Δ notation.

HRRs were calculated using a modified model based on that of Olanrewaju et al. [39] to provide a representation of the Yanmar L100V engine. The model modifications included the L100V engine geometry and the use of a single fuel injection. The first law of thermodynamics was used in the derivation of the model. It assumes the charge is an ideal gas in a single zone and is zero-dimensional. The model has terms to account for blow-by losses, evaporative losses, and heat losses to the wall. A second-order Savitzky-Golay filter was applied with a five-point window to reduce the noise in the P-CA traces [40].

The emissions analysed and the appropriate sampling methods are summarised in Table 4. Here we measured $PM_{2.5}$, defined as the mass of particulate matter (PM) per unit volume of air passing a size-selective inlet with a 50% cut point efficiency at 2.5 µm aerodynamic diameter. The $PM_{2.5}$ was measured using a direct sampling methodology without dilution to ensure that within the short tests enough $PM_{2.5}$ was collected such that the masses could be determined reliably and accurately. Total PN and particle number size distributions (PNSDs) for particles with diameters between 4 – 1000 nm were measured using a Cambustion DMS500 held at 55 °C. The specific emissions for each fuel were calculated using ISO 8178 weighting factors and were compared to the Euro Stage V limits [37,38]. Where there was no data at the required loads for calculating the emissions factors, values were calculated from fitting the measured data and then used in the ISO 8178 calculation [38].

Table 4. Emissions analysis techniques and analysers.

Emission	Detection Technique	Analyser	Analyser Sensitivity
CO	Non-Dispersive Infrared	MEXA 7100D	1 ppm for low range, 0.01 vol% for high range
THC	Flame Ionisation Detection		1 ppm
NO_X	Chemiluminescence		1 ppm
$PM_{2.5}$	Particulate separating cyclone and glass fibre filter papers	Modified Single Stage Andersen Sampler	Balance Accuracy: 0.01 mg Cyclone 50% cut point efficiency
PN	Electrical Mobility	Cambustion DMS500	Detection limit of 2×10^4 #/cm^3
Volatile Organic Compounds	Fourier Transform Infrared Spectroscopy	Gasmet DX4000	Calibration ranges: Formaldehyde: 0 – 200 ppm. Acetaldehyde: 0 – 100 ppm.

3. Results and Discussion

3.1. Influence of Butyl-Based Blends on Engine Performance

3.1.1. Influence of Blend Composition on Ignition Delays

IDs in the engine are not only influenced by the chemical autoignition of the fuel, but also by the physical processes of fuel vaporisation and turbulent mixing which are influenced by changes in the fuel's physical properties [21]. At all loads tested, the IDs increased relative to the ULSD baseline. The IDs were up to 2.5 CAD longer than diesel, as shown in Fig. 1. IDTs were up to 12% longer (Appendices A1.1), depending on the blend composition.

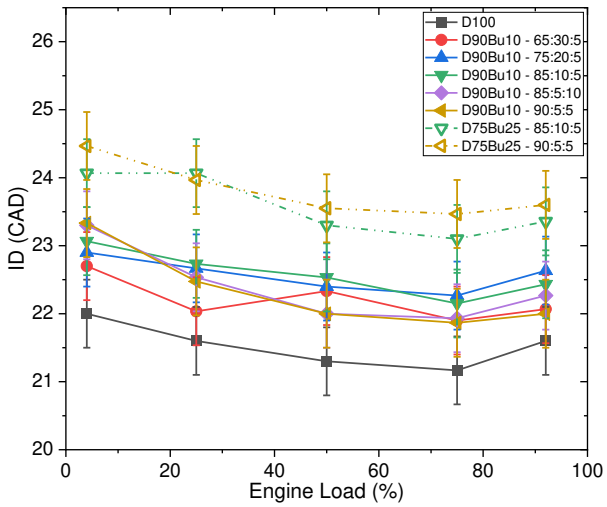

Figure 1. Ignition delays in CAD for the butyl-based blends and diesel.

We might expect IDs to increase in-line with the *n*BL fraction in the blends, since it has the lowest DCN of all the fuel components (Table 1), and is present in the highest blend fractions. However, this is not an obvious feature of the data across all engine loads above 4%. IDs may also be influenced by competing effects related to the high DCN of DNBE (increasing reactivity), and the charge cooling effects of DNBE and *n*BuOH (reducing reactivity). Fig. 1 shows that the blend with the highest *n*BL fraction (D90Bu10 – 90:5:5) actually has the shortest ID out of the 10 vol% blends despite having the lowest blend DCN (Table 2) [22]. Kim et al. [21] demonstrated that density can influence the ID of a fuel. However, the densities of all Bu10 blends are within 1% of each other (Table 2), and are therefore an unlikely influence in this case. The longest ID at high loads out of the 10 vol% blends occurs for the D90Bu10 – 75:20:5 blend i.e. one with a substantial amount of DNBE. Also, when comparing the 10 and 25 vol% blends of the same composition, the changes in the IDs of the 25 vol% blends were not 2.5 times greater than those of the 10 vol% blends at all loads, as would be predicted by a linear response to the biofuel fraction relative to diesel (Appendices A1.1 and Table A1.1.3). Therefore, the results show a non-linear relationship between the biofuel fraction and ID, which may be related to changes in the non-standardised physical and chemical properties such as enthalpy of vaporisation and specific heat capacity. In particular, charge cooling effects of the highly volatile DNBE may play a significant role [21]. Hence, blends with the lowest DCN due to the high *n*BL fraction did not show proportional increases in IDs in the engine, due to the influence of other physical properties [21,22].

The longer IDs of the biofuel blends will influence engine performance and emissions when compared to the diesel baseline. The engine performance parameters influenced by ID include peak

in-cylinder pressure, which will then affect power output, thermal efficiencies, and thus BSFC. Longer IDs will also affect fuel/air mixing times, potentially leading to fewer in-cylinder rich zones where PM is typically produced [41]. On the other hand, longer IDs reduce residence times required for the oxidation of particulates and their precursors as well as potentially increasing CO and THC emissions formed from incomplete combustion [41-43]. These features will be discussed in the following sections.

3.1.2. Influence of Blend Composition on In-Cylinder Peak Pressures

The butyl-based blends led to smaller changes in peak in-cylinder pressures compared to diesel as the engine load increased (Fig. 2). Some blends could match the peak pressure produced with diesel at higher loads. The higher loads are the typical operational window of a genset, so maintaining peak pressure at these loads should contribute to maintaining engine performance when using the biofuel blends. Some butyl-based blends produced in-cylinder peak pressures that were within one standard error of the diesel peak pressure, namely: D90Bu10 – 65:30:5, 75:20:5, and 85:10:5. These blends had the shortest IDs of the butyl-based blends and hence the combustion occurred earlier in the piston cycle, closer to the timing of D100, at a higher in-cylinder pressure. Lower pressures could reduce NO_X emissions, as in-cylinder temperatures would also be reduced [41,44,45]. However, lower temperatures may increase CO, HC, and PM emissions due to less complete combustion. Additionally, lower in-cylinder pressures could reduce engine power output (e.g. IMEP) and engine efficiency, thus increasing fuel consumption. The influence of the biofuel blends on the fuel consumption is discussed in the next section.

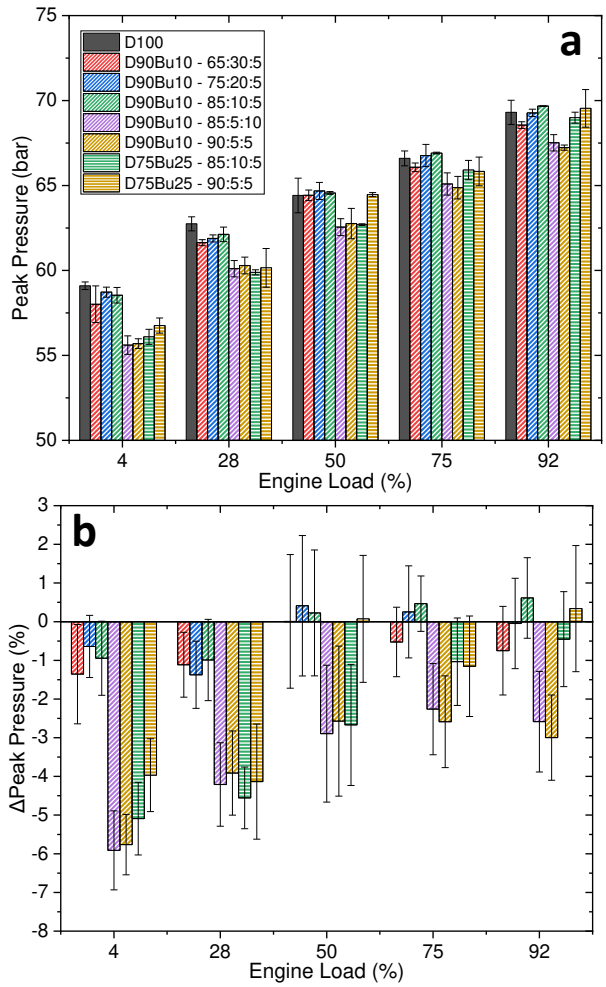

Figure 2. a – Peak pressures for the butyl-based blends and D100. b – Changes in the peak pressure for the butyl-based blends relative to D100.

The peak pressure reductions may be alleviated if modifications such as advanced injection timing or a cetane number enhancer, such as 2-ethylhexyl nitrate, were made to overcome the longer IDs [5]. These could be potentially cost-effective solutions that may increase the possibility of utilising these fuel blends. However, the influence of such changes would require further study.

3.1.3. Influence of the Biofuel Blends on Brake Specific Fuel Consumption

One of the main concerns for end users when changing fuel, particularly with oxygenated advanced biofuels, is the potential for increased fuel consumption. Therefore, the BSFC of the biofuel blends needs to closely match that of diesel. The Yanmar L100V fuel delivery system operates on a volumetric basis. Therefore, any changes in fuel density change the mass of fuel injected, which results in the stoichiometry changing [46,47]. Changes in the elemental composition, energy content, and fuel density were not accounted for in the engine operation, as the aim was to establish if the biofuel blends could be used without any engine modifications. At higher engine loads, more fuel is consumed on a mass basis compared to lower loads, but the BSFC reduces since thermal efficiency is increased at higher loads.

The BSFC increased with increasing *n*BL fraction (Fig. 3) due to decreasing LHVs (Table 2). For the 10 vol% blends, the increases in BSFC were within one standard error of the diesel baseline, demonstrating that there was no statistically significant penalty for fuel consumption when running with these blends. The increase in the BSFC for the 25 vol% blends was not 2.5 times greater than those of the corresponding 10 vol% blends. The increase in BSFC was greater than the reduction in LHVs for both 25 vol% blends, as the reduction in LHV was 9%, yet the BSFC increased by more than 10% at all loads. This larger increase indicates that the increased density, longer IDs, higher enthalpy of vaporisation, and lower LHVs produced less power, increasing the BSFC. One possible reason for this disproportionate increase is an extended diffusion combustion phase due to the lower LHVs and longer IDs. Therefore, the 10 vol% blends could be more favourable in terms of maintaining fuel economy in engines similar to the Yanmar L100V. They would however, offer lower potential CO_2 savings. Of the two 25% biofuel blends, that with the higher DNBE fraction compared to *n*BuOH (D75Bu25 – 85:10:5), offered the best fuel efficiency.

Whilst the aim of this work was to assess the fuel blends as drop-in fuel, there are several operational parameters that could be optimised to overcome the increase in BSFC. One of which changing the fuel injection timing. The injection timing would need to be earlier to account for the longer ID. On the Yanmar L100V engine this requires manually adjusting the flywheel. In an engine with an engine control unit (ECU) this would require the ECU to be recoded to change the injection timing. A second parameter would be to increase the fuel injection pressure to improve the atomisation of the fuel, creating smaller droplets that would more readily vaporise, and thus ignite with shorter IDs. Optimising either of these parameters would ensure the peak pressures are not reduced (Fig 2), and the power generated by the engine when running with the biofuels is maintained at the same level as the diesel.

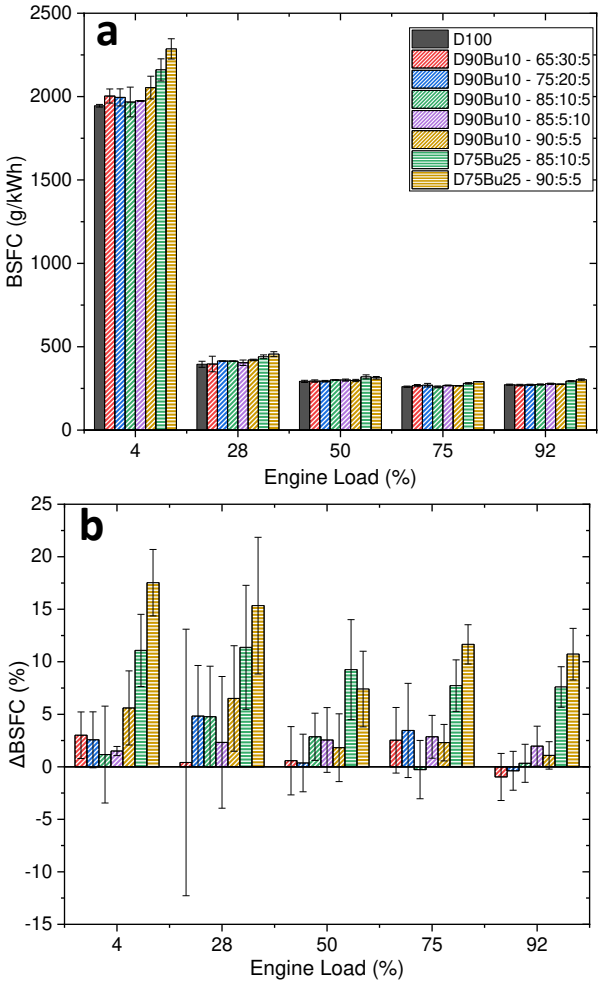

Figure 3. a – BSFC for the butyl-based blends and D100. b – Changes in the BSFC for the butyl-based blends relative to D100.

3.1.4. Influence of the Biofuel Blends on Heat Release Rates

Derived HRRs for selected blends from Table 2 at 50% and 92% load are shown in Figs. 4 and 5. The 92% load tests were chosen as the engine would typically run at this load in a real world setting, and the 50% load was chosen as a lower load with a higher engine speed. HRRs are influenced by IDs, energy content, specific heat capacity, and other fuel properties. Therefore, we would expect competing effects following the addition of the three-component biofuel blends with differing component fractions when mixed with diesel.

For all of the butyl-based blends, there was an increase in peak HRR at 92% load, whereas, at 50% load, there was a reduction. At both load conditions, the timing of peak HRR was delayed, with a greater delay at the lower load. The changes in the peak HRRs at 92% load follow the same pattern as those for the IDs for these fuel blends, i.e. longer IDs lead to higher peak HRRs. These changes are likely to also be caused by competing effects of changes to different fuel properties of the fuel blend components. The longer IDs are likely to have increased mixing time, and therefore also the proportion of the fuel undergoing ignition under premixed conditions, leading to a greater peak HRR [22,48]. Increases in peak HRR have also been reported for fuel blends with longer IDs in the study of Jamrozik [48] for diesel and ethanol blends, where increasing the ethanol fraction increased peak HRRs. This increase was also suggested to be due to the increase in premixed combustion due to the lower DCN of ethanol, resulting in longer IDs [22,48].

Increasing the biofuel fraction to 25 vol% also caused the premixed combustion phase to be broader, as shown in Fig. 5. This broadening was likely due to the high enthalpy of vaporisation and high boiling point of *n*BL since it is present in large fractions of the total fuel blend. Increases in the proportion of fuel combusted under premixed conditions is expected to have a beneficial impact on PM emissions, which will be explored in the next section. It will also be important to explore the impact of these changes on NO_X emissions as increasing peak HRR, whilst being beneficial for power output, could also increase in-cylinder temperatures, potentially leading to increased NO_X emissions [41,44,45].

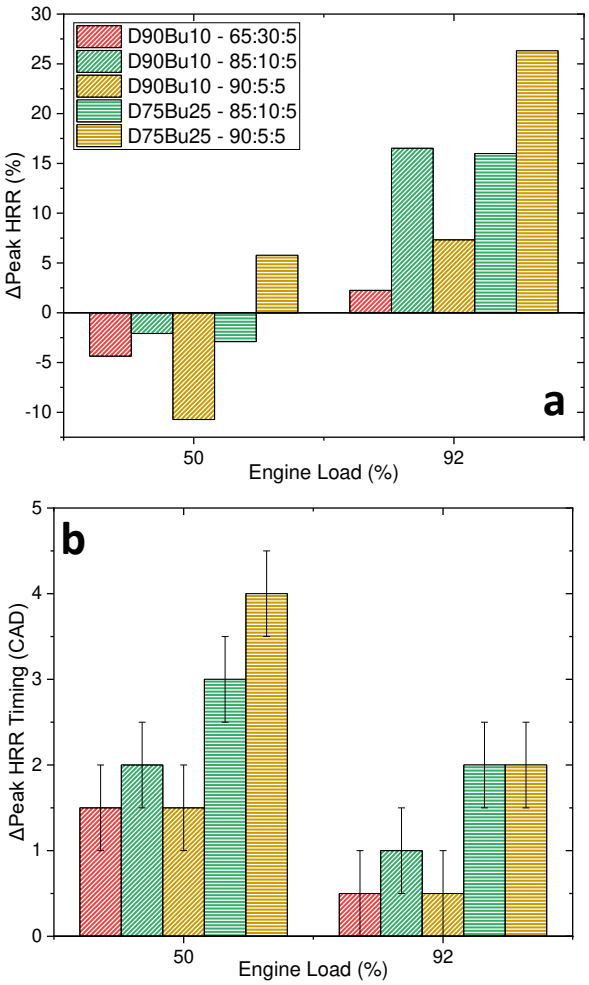

Figure 4. a – changes in peak HRR for the butyl-based blends relative to D100. b – Changes in the timing of peak HRR for the butyl-based blends relative to D100.

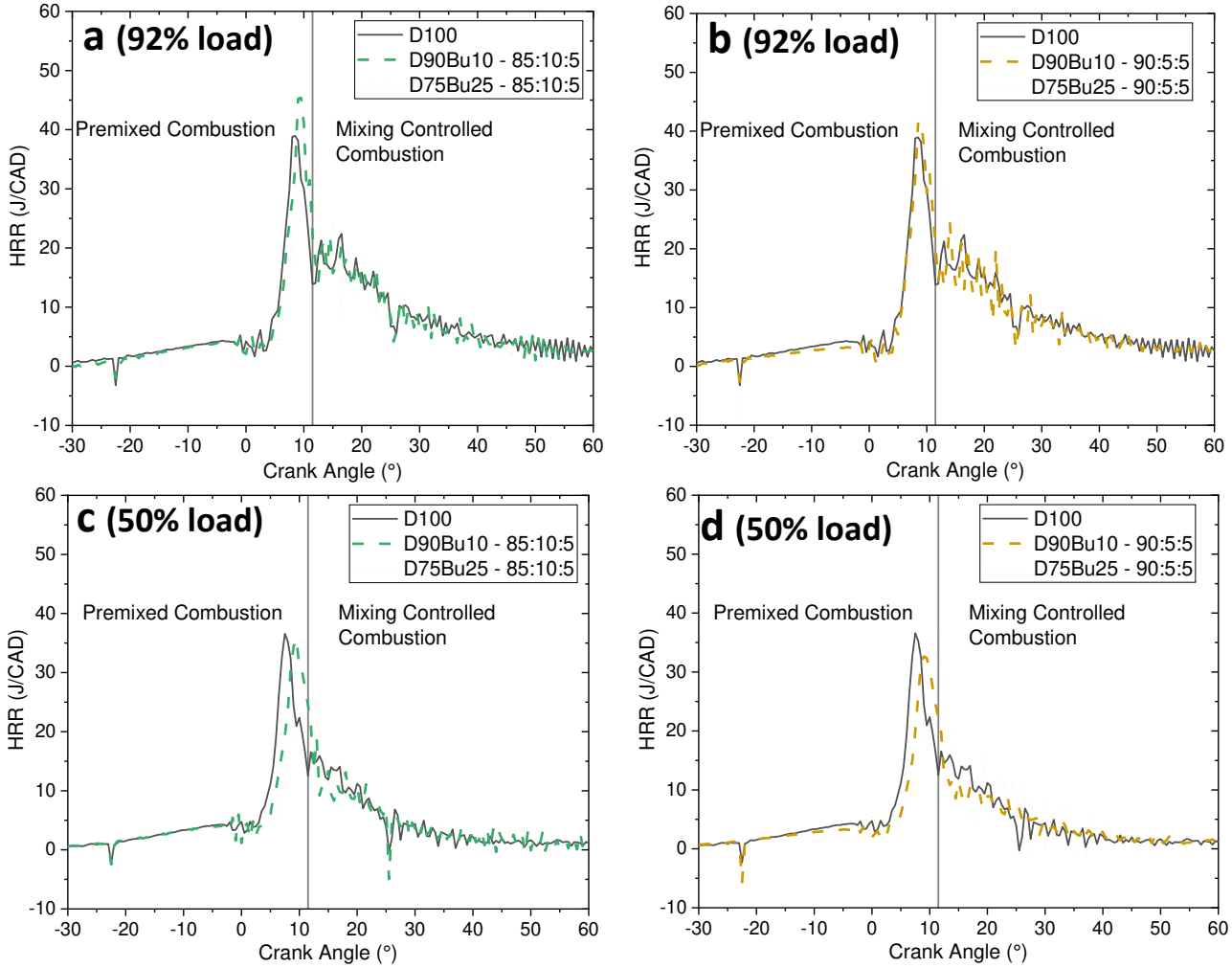

Figure 5. HRR curves for the selected butyl-based blends with 10 and 25 vol% blends, where a & b are at 92% load for butyl-three component blends 85:10:5 and 90:5:5, respectively, and c & d are at 50% load for butyl-three component blends 85:10:5 and 90:5:5, respectively. Vertical line in each figure indicates the start of mixing controlled combustion for D100.

3.2. Influence of Butyl-Based Blends on Engine Out Emissions

3.2.1. Influence of the Biofuel Blends on Regulated Gaseous Emissions

Emissions of THC and CO in g/kWh for the different fuel blends, at different engine loads, are shown in Figs 6a,b and 7a,b respectively, with differences relative to D100 (ΔTHC and ΔCO) shown in Figs. 6c and 7c. The ΔTHC decreased as engine load increased to become negative at 92% load (Fig. 6c), indicating a reduction in THC emissions compared to diesel. At <50% load, there was a correlation between the increase in THC emissions and the increasing *n*BL fraction (Fig. 6c). The reduction in THC emissions at the higher loads is a positive outcome for the butyl-based blends as the high combustion temperatures, due to *n*BL's high adiabatic flame temperature, mitigates the effects at high load of the lower DCNs compared to ULSD due to *n*BL's low DCN [22]. Additionally, gensets typically operate at >50% load, and a reduction in THC emissions could improve local air quality in regions where gensets are used for power generation.

Fig. 7c shows the changes in CO emissions due to the addition of the butyl-based blends. They show the same trend as THC emissions, where the increase in CO emissions reduced as the engine load increased, with one blend even showing a reduction at the highest load. There was a correlation between both the total biofuel fraction, and the *n*BL fraction in the blend, and the increase in CO emissions. Lower *n*BL and higher DNBE led to the most favourable changes in ΔCO. This was likely due to the high DCN of DNBE promoting complete combustion.

Since NO_X emissions are temperature dependent, the peak HRR and its timing will affect the in-cylinder temperature and thus NO_X emissions [41]. NO_X emissions were reduced at loads <92% for the blends with high DNBE fractions, as shown in Fig. 8. At 92% load, D90Bu10- 65:30:5 showed a reduction in NO_X emissions. A possible explanation for this may be that the large DNBE fraction had a greater charge cooling effect due to its high volatility compared to the other butyl-based components (Table 1) [21]. Additionally, the low *n*BL fraction would have contributed to maintaining low NO_X emissions, as the combustion temperatures would be lower than for the high *n*BL blends.

The increase in NO_X emissions with D75Bu25 – 90:5:5 (Fig. 8b) may be due to a combination of the greater peak HRR, and *n*BL's high adiabatic flame temperature compared to the other components (Table 1), increasing thermal NO_X relative to ULSD and blends with low *n*BL fractions [41]. Although the increases were small, if such fuels were used in transport vehicles, tests would need to be conducted to establish whether exhaust after-treatment systems would be sufficiently effective to control tailpipe NO_X emissions [36,41,49].

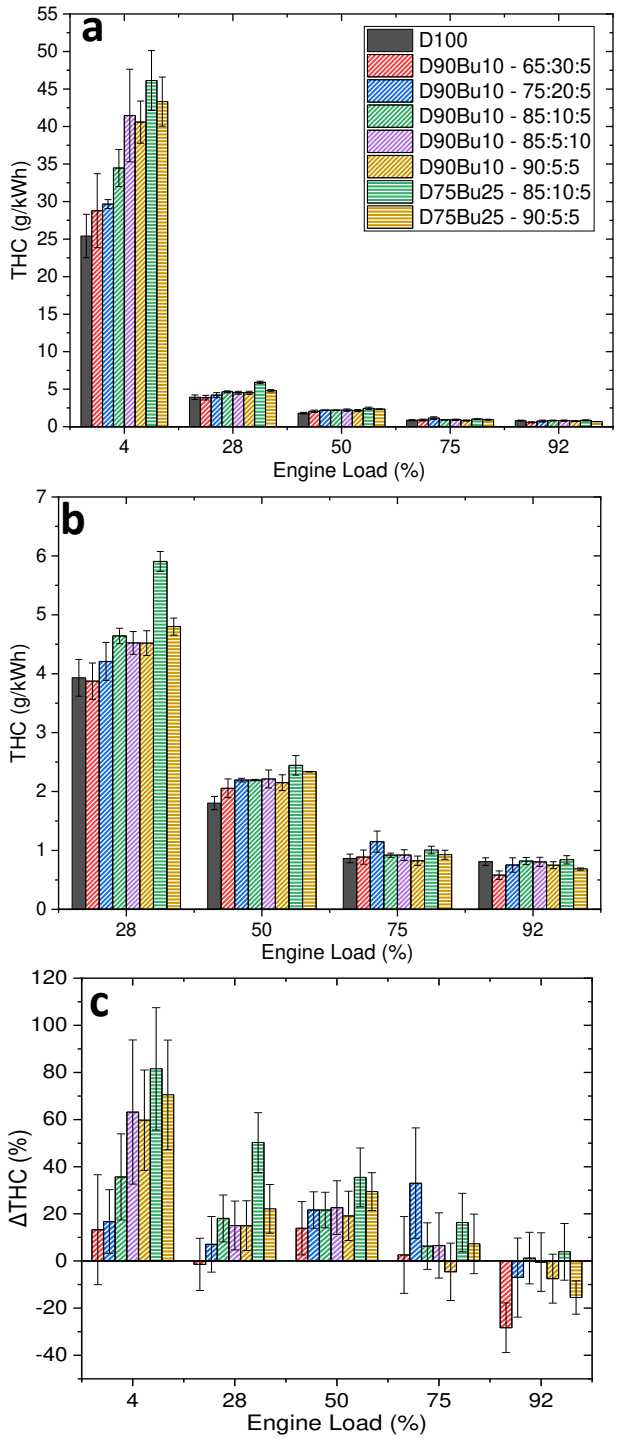

Figure 6.a – THC emissions at all engine loads tested for all fuels tested. b – THC emissions at engine loads above 4% for all fuels tested. c – Change in THC emissions relative to D100 baseline.

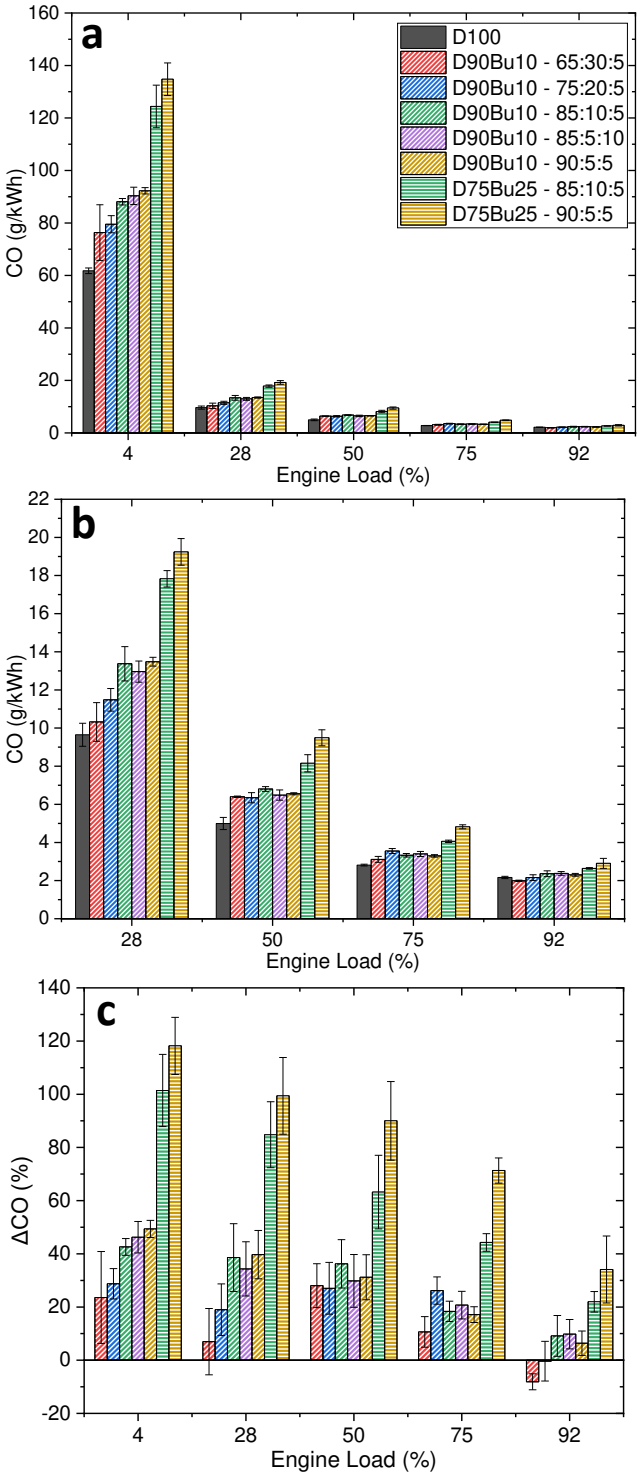

Figure 7. a – CO emissions at all engine loads tested for all fuels tested. b – CO emissions at engine loads above 4% for all fuels tested. c – Change in CO emissions relative to D100 baseline.

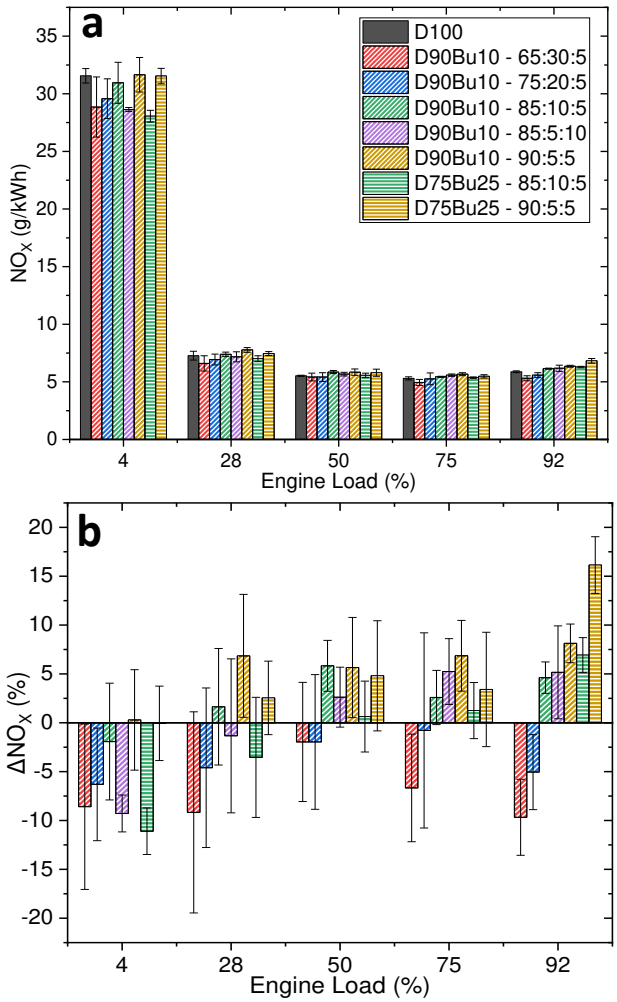

Figure 8. a – NO_X emissions at all engine loads tested for all fuels tested. b – Change in NO_X emissions relative to D100 baseline.

3.2.2. Influence of the Biofuel Blends on Non-Regulated Gaseous Emissions

Non-regulated emissions from CI engines (such as aldehydes for example) can also have negative impacts on air quality and public health due to, for example, their ozone formation potential and carcinogenicity [50-52]. The concentrations of these species in exhaust gases are commonly reported to increase when using oxygenated biofuels including for the butyl-based blend components tested here [50,53-56]. In addition, there is the possibility that formaldehyde will be included in the Euro 7 vehicle exhaust emission standards as the standard states [36]:

'*By 31 December 2027, the Commission shall conduct a review on the appropriateness of setting out a specific limit for formaldehyde emissions in respect of vehicles of categories M2, M3, N2 and N3 based on the expected use of fuels that would lead to an increase in formaldehyde emissions*'.

The vehicle categories mentioned above relate to larger vehicles such as busses, lorries, and other heavy-duty road going vehicles which typically use diesel fuels. Therefore, it is important to understand the potential impact of new potential fuel blend characteristics on formaldehyde emissions.

Fig. 9 shows exhaust concentrations of formaldehyde and acetaldehyde for five engine loads across the different fuel blends. As the engine load increased, concentrations of formaldehyde decreased (Fig. 9a), whereas, acetaldehyde concentrations remained similar for loads above 4%. The addition of the butyl-based blends increased both aldehyde concentrations at low load, correlating with increasing *n*BL fraction in the blend. The increased formation at low load is due to the lower in-cylinder pressures (Fig. 2a) and resultant lower in-cylinder temperatures. Formaldehyde is a stable oxidation product from both high and low temperature combustion of *n*BuOH [57]. These results also indicate that *n*BL combustion results in formaldehyde production, as the *n*BuOH content in most blends is fixed and the formaldehyde emissions correlate with the *n*BL fraction of the blend. At 92% load, the formaldehyde concentrations are similar to the diesel baseline value, with a slight reduction for the Bu10 blend with 65% *n*BL, and slight increases for the Bu25 blends. However, they were all within on standard deviation of the diesel baseline. Since the genset would normally operate at maximum load, the use of the butyl-based blends is not expected to increase formaldehyde emissions. For transport applications, after-treatment systems, such as diesel oxidation catalysts (DOCs), should oxidise and remove formaldehyde but careful design of exhaust aftertreatment systems is needed for avoiding detrimental impacts on air quality as exhaust temperatures are relatively low at low load.

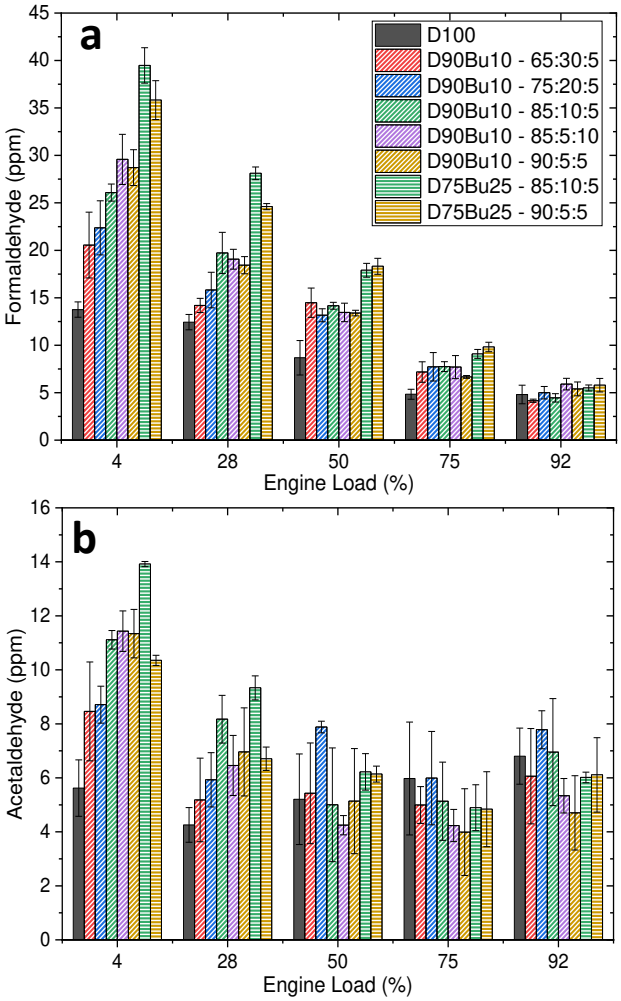

Figure 9. Average concentrations in exhaust gas for all fuels tested for a – formaldehyde and b – acetaldehyde.

Acetaldehyde concentrations (Fig. 9b) show a similar trend to those of formaldehyde, although above 50% engine load the biofuel blends show similar concentrations to diesel, and in some cases lower. Lower concentrations occur for fuels with only 5 vol% DNBE in the three-component blends. The possibility to maintain, or even reduce acetaldehyde emissions at high load relative to diesel, is potentially beneficial in terms of air quality impacts.

3.2.3. Influence of the Biofuel Blends on the Particulate Emissions

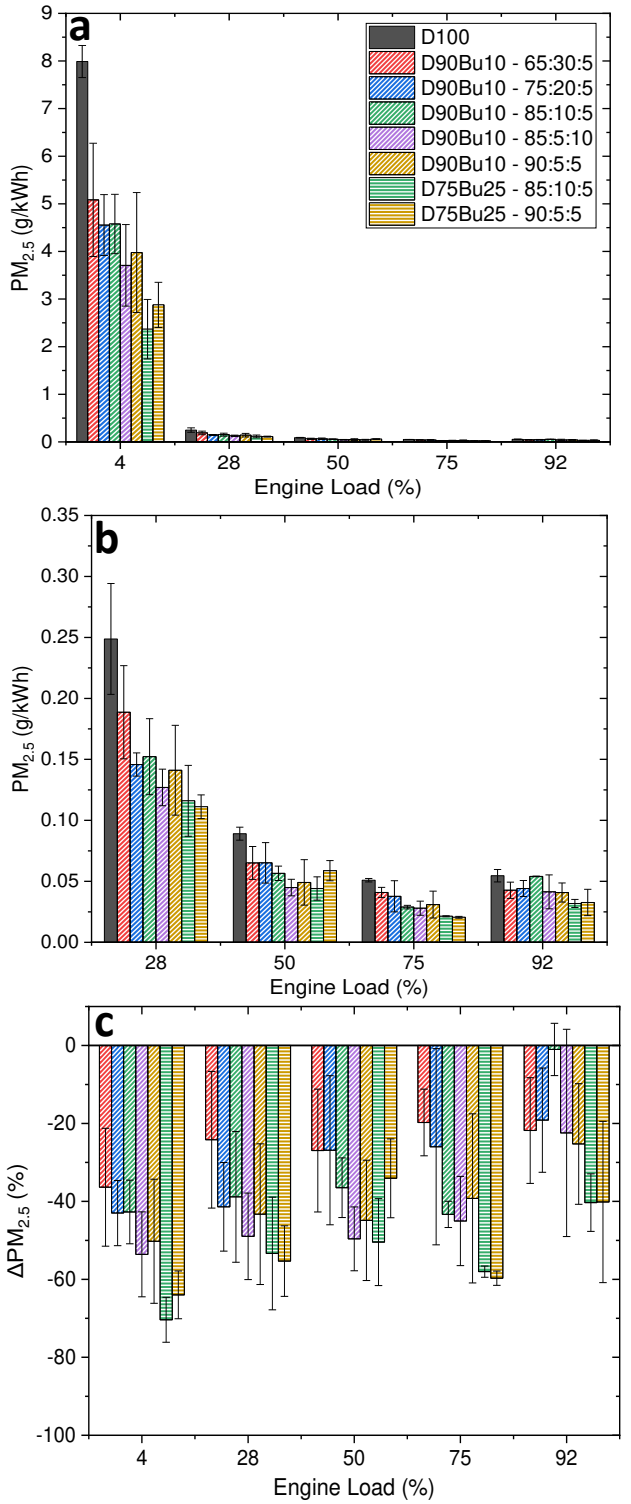

Figure 10. a – $PM_{2.5}$ emissions at all loads tested for all fuels tested. b – $PM_{2.5}$ emissions at engine loads above 4% for all fuels tested. c –Change in $PM_{2.5}$ emissions relative to D100 baseline.

Use of the butyl-based blends caused a substantial reduction in $PM_{2.5}$ emissions of up to 70% relative to diesel. This reduction was correlated with the *n*BL fraction in the biofuel blend (Figs. 10a-c) and thus shows the opposite trend to gaseous emissions, which reduced with increasing DNBE fraction. The reduction in $PM_{2.5}$ relative to diesel follows trends commonly observed for the utilisation of oxygenated biofuel blends, such as the reduction in FSN, observed by Antonetti et al. [12] and Frigo et al. [11] when testing butyl-based blends. At higher loads, more total $PM_{2.5}$ was generated throughout the test compared to lower loads due to more fuel being consumed.

The addition of the butyl-based blends resulted in a consistent reduction in particle number (PN) as well as mass emissions for most blends at all powers (Figs. 11b&c). The PN reduction at all loads, with D75Bu25 – 90:5:5 was less than for the other blends. Since the PN measured was the total PN, there is the potential that with high *n*BL fractions there were droplets of condensed unburnt fuel and semi-volatile particles being measured, as the boiling point of *n*BL is 237 °C and the DMS500 was held at 55 °C. The reductions in PN were higher than those for the mass based $PM_{2.5}$ measure, indicating the potential additional effect of agglomeration processes.

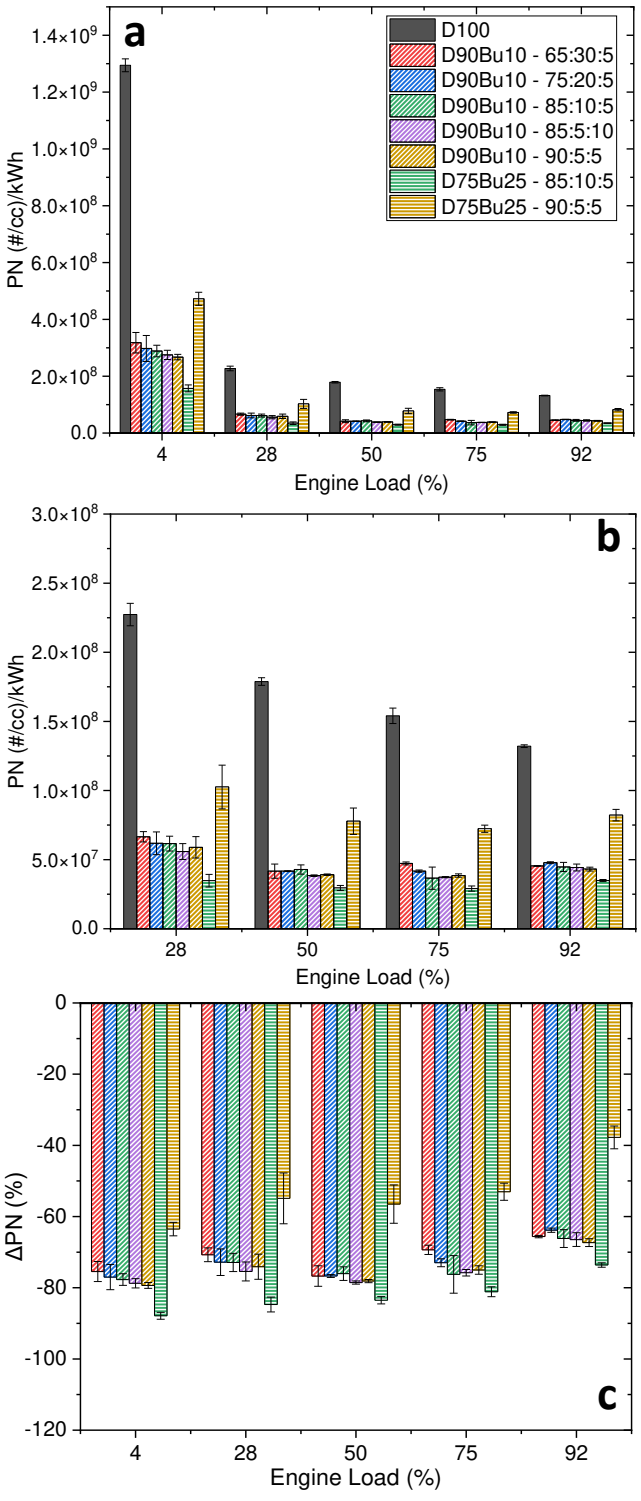

Figure 11. a – PN emissions at all engine loads tested for all fuels tested. b – PN emissions at engine loads above 4% for all fuels tested. c – Change in PN emissions relative to D100 baseline.

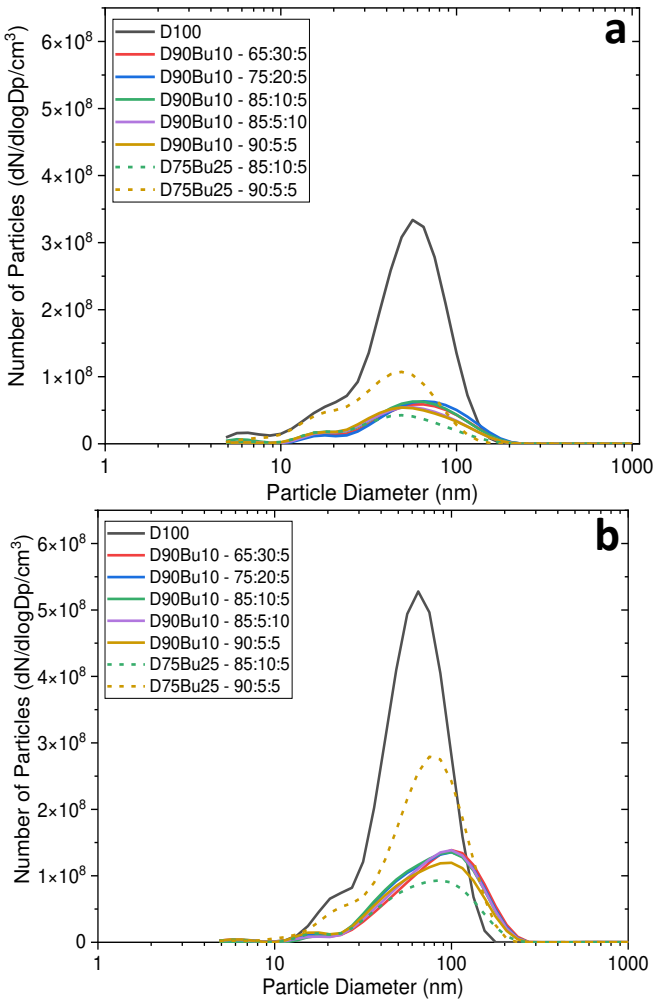

Figure 12. PNSDs for the different fuel blends at a – 50% load and b – 92% load.

Fig. 12 shows the particle number size distributions (PNSDs) for the different biofuel blends. Several peaks in the curves demonstrate a multi-modal distribution, with peaks present below 10 nm, around 18 nm and around 60 nm (the largest peak) for the D100 baseline. The area under the PNSD curve represents the total PN and reduces on addition of the biofuel blends in line with the data shown in Fig. 11. The shape of the curve also changes on the addition of the biofuel blends however, showing an increase in the peak particle size, particularly at the higher load (Fig. 11b). At 92% engine load, the peak diameter increased to around 100 nm for the biofuel blends compared with 60 nm for the D100 baseline. Again, this is indicative that agglomeration or enhanced condensation processes have occurred for the biofuel blends shifting the main particle diameter peak towards larger diameters. The larger diameter particles would be formed when higher numbers of smaller particles agglomerate or there is increased condensation of particle precursors to form the larger particles.

3.2.4. Causes for the Change in Emissions

The longer IDs from addition of the butyl-based blends (Fig. 1) result in ignition occurring further away from top dead centre, reducing maximum in-cylinder pressures (Fig. 2) and thus likely also temperatures. Longer IDs also reduce the time available for combustion to complete, leading to increased CO and THC emissions. It was expected that there would be an increase in particulate emissions due to less complete combustion. However, it is likely that there was increased premixed combustion due to the longer IDs, as shown by the increased peak HRR (Figs. 4 and 5). This potentially reduced the number of rich zones within the cylinder, where particles are typically produced [11]. The longer IDs also contributed to maintaining NO_X emissions reasonably close to the diesel baseline, by reducing the influence of the high adiabatic flame temperature of *n*BL (Table 1). Longer IDs typically reduce local equivalence ratios, reducing particle formation, but this usually has the trade-off of increasing local temperature, thus increasing NO_X formation. However, this is not what was observed when using the butyl-based blends [58,59]. Therefore, the synergistic effect of high enthalpies of vaporisation and longer IDs, potentially countered the higher adiabatic flame temperatures thus contributing to the control of NO_X emissions.

In addition to increased premixed combustion, the oxygen fraction in the fuel blend increases upon the addition of the biofuel blends. For the butyl-based blends, the O/C ratios for the 10 vol% biofuel blends ranged from 0.044 to 0.049 as the *n*BL content increased. This increase in the O/C ratio caused the reduction in PN to be greater for the blends with higher *n*BL fractions. The addition of the biofuel blends also reduced the aromatic content of the blend relative to ULSD, likely reducing the production of soot precursors.

3.2.5. Specific Emissions

The emissions standard applicable in this work is Euro Stage V, with the limits displayed in Table 5 [37].

Table 5. Euro Stage V CI genset emissions limits [37]. PM is particulate matter.

Engine Power (kW)	CO (g/kWh)	NO_X+THC (g/kWh)	PM (g/kWh)	PN (#/kWh)
0<P<8	8.0	7.5	0.6	-

Table 6 shows the calculated specific emissions for the butyl-based blends with the EU Stage V emissions standard, where PM emissions are represented by $PM_{2.5}$ measured using the non-standard method described in Section 2.2. Since the testing methodology used was non-compliant with ISO 8178, the comparison to the EU Stage V limits is to highlight the influence of the biofuel blends on the emissions [37,38]. The emissions factors were determined using the analysis techniques summarised in Table 4. The errors presented in Table 6 were calculated by propagating the errors of the specific emissions at each load required for the calculation of the overall specific emission according to ISO 8178 [38]. It shows that the engine was compliant for PM, but not for CO and NO_X+THC for all fuel blends, including diesel, demonstrating that the limits derived from standard test procedures do not necessarily reflect real world operation.

Table 6. Specific emissions for the butyl-based blends

Blend	CO (g/kWh)	NO_X+THC (g/kWh)	$PM_{2.5}$ (g/kWh)	PN (#/kWh)
Stage V limits	8.0	7.5	0.6 (PM Limit)	-
D100	8.2 ± 0.5	11.6 ± 0.8	0.49 ± 0.09	(2.5 ±0.4)×10^8
D90Bu10 – 65:30:5	9.4 ± 1.0	11.1 ± 1.5	0.34 ± 0.08	(6.9 ±1.0)×10^7
D90Bu10 – 75:20:5	10.1 ± 0.6	11.7 ± 1.0	0.29 ± 0.06	(6.5 ±1.3)×10^7
D90Bu10 – 85:10:5	11.3 ± 0.8	12.7 ± 1.1	0.30 ± 0.07	(6.4 ±1.1)×10^7
D90Bu10 – 85:5:10	10.9 ± 0.7	12.4 ± 1.1	0.23 ± 0.06	(5.9 ±0.9)×10^7
D90Bu10 – 90:5:5	11.1 ± 0.7	12.9 ± 1.0	0.25 ± 0.08	(6.0 ±0.8)×10^7
D75Bu25 – 85:10:5	14.7 ± 1.3	13.5 ± 1.0	0.18 ± 0.05	(3.8 ±1.5)×10^7
D75Bu25 – 90:5:5	15.6 ± 1.7	13.0 ± 1.3	0.19 ± 0.07	(1.1 ±0.2)×10^8

Due to the weighting factors used in ISO 8178, all of the biofuel fuel blends tested resulted in non-compliant CO and NO_X+THC emissions, even though there were reductions in THC and CO emissions for some blends at higher loads [38]. The main contributor to the increases in the NO_X+THC specific emissions were the increases in THC emissions at low loads. To control the increases in CO and THC several strategies are possible such as i) the optimisation of the engine operation, through for example, advanced injection timing to compensate for the longer IDT, ii) the

addition of an additive to enhance the DCN of the blend, iii) installation of a DOC to control exhaust emissions [60]. The use of gensets is a major contribution to air pollution in many cities worldwide and the use of exhaust after-treatment systems for all fuels would reduce this impact. However, it is also worth noting that real world operation is usually at high loads where the THC in fact reduced relative to diesel. In addition, the use of biofuel blends could limit the need for after-treatment to gaseous emissions only, due to the large reductions in PM compared to diesel.

4. Conclusions

Seven different butyl-based tertiary biofuel blends that meet the density, kinematic viscosity and flash point requirements of the existing fuel standards, were tested for engine combustion performance and emissions to investigate their suitability as low-carbon alternatives to diesel. All blends showed stable operation within the test engine and demonstrated the potential for minimal changes in emissions if the fuel blend was tailored to standard property limits. The relative changes in the engine performance for the different blends indicate that the butyl-based blends have the potential to be suitable low-carbon alternatives to diesel. The key findings are summarised as follows:

- Efficiency penalties, which are typically associated with using fuels with high oxygen fractions, were not found to be too severe when using the biofuel blends. At high engine load, the BSFC did not increase significantly compared to D100 when running the 10 vol% butyl-based blends. The changes in BSFC and peak pressure for the Bu10 blends were within one standard deviation of the diesel baseline. These changes may be an acceptable tolerance for the users of similar engines. This close match in performance for the butyl-based blends with diesel indicates that these biofuels can be used as drop-in fuels without adverse impacts on an engine's operational performance.
- Ignition delays increased following the addition of the butyl-based blends. IDs would expect to be influenced by changes to the DCN of the blends but did not follow a linear increase when increasing the biofuel fraction from 10 vol% to 25 vol% indicating the influence of other non-standardised physical properties such as enthalpy of vaporisation and specific heat capacity. Charge cooling effects of DNBE are thought to be significant. Changes in ignition delays influenced engine-out emissions due to the resulting changes in peak HRR and pressure as well as increased mixing time of the fuel air mixture.
- Addition of the butyl-based blends caused increases in CO and THC emissions, particularly at lower loads, which are consistent with previous studies using high *n*BL fractions blended with diesel. NO_X emissions were maintained relative to diesel when using the butyl-based blends except for at high engine loads with a high *n*BL fraction in the fuel blend.
- All butyl-based biofuel blends showed significant reductions in $PM_{2.5}$ and PN emissions relative to D100. This was likely to be due to an increased premixed combustion phase along with the reduction in the aromatic content in the final fuel blends as well as increases in the fuel oxygen fraction. Changes in the particle size were also seen, corresponding to an increase in larger agglomerates resulting in larger reductions in particle number emissions compared to mass based emissions for the biofuel blends relative to diesel.
- The presence of DNBE was beneficial for the performance and engine-out emissions of the butyl-based blends due to its higher DCN than the other biofuel components. The blends with higher DNBE fractions showed lower increases in CO and THC across all load settings, with some reductions at the highest load. These blends also showed reductions in NO_X emissions. Reductions in PN and NO_X could facilitate meeting future lower emissions standard limits, without reliance on exhaust after-treatment systems – or at least limit those to gaseous emissions.

Overall, the butyl-based blends showed promise as low-carbon alternatives to diesel, and thus could have the potential to displace fossil-based diesel within gensets. They may also have wider applications within the transport sector and thus contribute to the RED II target. However, they would have to be produced using feedstocks that comply with Annex IX of RED II, such that they would contribute towards the 3.5% advanced biofuel blending target for transport fuels. This could be possible using acid catalysed alcoholysis methods using lignocellulosic feedstocks [13]. Being able to use high fractions of *n*BL in the butyl-based blends would enable the contribution to match, if not exceed, the 3.5% target [6]. Testing the use of these fuels in transient operation, under varying loads, will also be required to determine their suitability for use in vehicles as a low-carbon diesel alternative. Additionally, optimisation of engine operation for use with different blend formulations, or the use of exhaust after-treatment systems, may be required to ensure all existing/future emissions limits are met for the particular engine type studied here.

Declaration of Competing Interest

The authors declare that they have no known competing financial interests or personal relationships that could have influenced the work reported in this paper.

Acknowledgements

This research was supported by UKRI EPSRC training grant, EP/L014912/1, regulated by the University of Leeds Centre for Doctoral Training in Bioenergy, and UKRI EPSRC Grant EP/T033088/1. The authors would also like to express thanks to Scott Prichard for technical support when running the research engine.

Appendices

The appendices contain engine performance parameter data, specific emissions data, tabulated values of the relative change data presented in the figures, and the PNSDs for the three other engine loads tested.

References

[1] International Energy Agency. 2022. *Transport*. Paris: IEA. https://www.iea.org/.

[2] Aslam, Zahida, Hu Li, James Hammerton, Gordon Andrews, Andrew Ross, and Jon C. Lovett. "Increasing Access to Electricity: An Assessment of the Energy and Power Generation Potential from Biomass Waste Residues in Tanzania." *Energies* 14 6 (2021): 1793.

[3] *Automotive fuels - Diesel - Requirements and test methods.* BS EN 590:2022. Milton Keynes: BSI. 2022.

[4] *Fuel oils for agricultural, domestic and industrial engines and boilers* BS 2869:2017+A1:2022. Milton Keynes: BSI. 2022.

[5] Christensen, Earl, Aaron Williams, Stephen Paul, Steve Burton, and Robert L. McCormick. "Properties and Performance of Levulinate Esters as Diesel Blend Components." *Energy & Fuels* 25 11 (2011): 5422-5428. 10.1021/ef201229j.

[6] The European Parliament and Council of the European Union. Directive (EU) 2018/2001 of the European Parliament and of the Council of 11 December 2018 on the promotion of the use of energy from renewable sources. European Union. 2018.

[7] Council of the EU, 2023, "Council and Parliament reach provisional deal on renewable energy directive," https://www.consilium.europa.eu/.

[8] Flannelly, Thomas, Stephen Dooley, and J. J. Leahy. "Reaction Pathway Analysis of Ethyl Levulinate and 5-Ethoxymethylfurfural from d-Fructose Acid Hydrolysis in

Ethanol." *Energy & Fuels* 29 11 (2015): 7554-7565. 10.1021/acs.energyfuels.5b01481.

[9] Howard, Mícheál Séamus, Gani Issayev, Nimal Naser, S. Mani Sarathy, Aamir Farooq, and Stephen Dooley. "Ethanolic gasoline, a lignocellulosic advanced biofuel." *Sustainable Energy & Fuels* 3 2 (2019): 409-421. 10.1039/C8SE00378E.

[10] Alamgir Ahmad, Khwaja, Mohammad Haider Siddiqui, Kamal K. Pant, K. D. P. Nigam, Nagaraj P. Shetti, Tejraj M. Aminabhavi, and Ejaz Ahmad. "A critical review on suitability and catalytic production of butyl levulinate as a blending molecule for green diesel." *Chemical Engineering Journal* 447(2022): 137550. https://doi.org/10.1016/j.cej.2022.137550.

[11] Frigo, Stefano, Gianluca Pasini, Gianluca Caposciutti, Marco Antonelli, Anna Maria Raspolli Galletti, Samuele Gori, Riccardo Costi, and Luigi Arnone. "Utilisation of advanced biofuel in CI internal combustion engine." *Fuel* 297(2021): 120742. https://doi.org/10.1016/j.fuel.2021.120742.

[12] Antonetti, C., S. Gori, D. Licursi, G. Pasini, S. Frigo, M. Lopez, J. C. Parajo, and A. M. R. Galletti. "One-Pot Alcoholysis of the Lignocellulosic Eucalyptus nitens Biomass to n-Butyl Levulinate, a Valuable Additive for Diesel Motor Fuel." *Catalysts* 10 5 (2020): 509. 10.3390/catal10050509.

[13] McNamara, Conall, Ailís O'Shea, Prajwal Rao, Andrew Ure, Leandro Ayarde-Henríquez, Mohammad Reza Ghaani, Andrew Ross, and Stephen Dooley. "Steady states and kinetic modelling of the acid-catalysed ethanolysis of glucose, cellulose, and corn cob to ethyl levulinate." *Energy Advances* 3 6 (2024): 1439-1458. 10.1039/D4YA00043A.

[14] Wiseman, Scott, Christian A. Michelbach, Hu Li, and Alison S. Tomlin. "Predicting the physical properties of three-component lignocellulose derived advanced biofuel blends using a design of experiments approach." *Sustainable Energy & Fuels* 7 21 (2023): 5283-5300. 10.1039/D3SE00822C.

[15] Wu, Peng, Changlin Miao, Xinshu Zhuang, Wuhuan Li, Xuesong Tan, and Tianhua Yang. "Physicochemical characterization of levulinate esters with different alkyl chain lengths blended with fuel." *Energy Science & Engineering* 11 1 (2023): 164-177. https://doi.org/10.1002/ese3.1320.

[16] Ramli, Nur Aainaa Syahirah, and Fadzlina Abdullah. "Study of Density, Surface Tension, and Refractive Index of Binary Mixtures Containing Alkyl Levulinate and n-Alcohol from 298.15 to 323.15 K." *Journal of Chemical & Engineering Data* 66 5 (2021): 1856-1876. 10.1021/acs.jced.0c00694.

[17] Wang, Jinglan, Lifang Sun, Pengpeng Luan, Yangyi Wu, Zhanjun Cheng, Zhao Zhang, Xiangen Kong, Haifeng Liu, and Guanyi Chen. "Effect of diesel blended with di-n-butyl ether/1-octanol on combustion and emission in a heavy-duty diesel engine." *Environmental Pollution* 311(2022): 119976. https://doi.org/10.1016/j.envpol.2022.119976.

[18] Lapuerta, M., J. J. Hernandez, J. Rodriguez-Fernandez, J. Barba, A. Ramos, and D. Fernandez-Rodriguez. "Emission benefits from the use of n-butanol blends in a Euro 6 diesel engine." *International Journal of Engine Research* 19 10 (2018): 1099-1112. 10.1177/1468087417742578.

[19] Górski, Krzysztof, and Marcin Przedlacki. "Evaluation of the Influence of Diethyl Ether (DEE) Addition on Selected Physicochemical Properties of Diesel Oil and Ignition Delay Period." *Energy & Fuels* 28 4 (2014): 2608-2616. 10.1021/ef4025036.

[20] Raspolli Galletti, Anna Maria, Gianluca Caposciutti, Gianluca Pasini, Marco Antonelli, and Stefano Frigo. "Bio-additives for CI engines from one-pot alcoholysis reaction of lignocellulosic biomass: an experimental activity." *E3S Web Conf.* 197(2020): 08005.

[21] Kim, Doohyun, Jason Martz, and Angela Violi. "Effects of fuel physical properties on direct injection spray and ignition behavior." *Fuel* 180(2016): 481-496. https://doi.org/10.1016/j.fuel.2016.03.085.

[22] Yanowitz, Janet, Matthew A. Ratcliff, Robert L. McCormick, J. D. Taylor, and M. J. Murphy. Compendium of Experimental Cetane Numbers. 2017.

[23] Linstrom, P.J., and W.G. Mallard, eds. *NIST Chemistry WebBook, NIST Standard Reference Database Number 69*. Gaithersburg MD, 20899: National Institute of Standards and Technology.

[24] Nikitin, E. D., A. P. Popov, N. S. Bogatishcheva, and M. Z. Faizullin. "Critical temperatures and pressures, heat capacities, and thermal diffusivities of levulinic acid and four n-alkyl levulinates." *Journal of Chemical Thermodynamics* 135(2019): 233-240. 10.1016/j.jct.2019.03.040.

[25] Çelebi, Yahya, and Hüseyin Aydın. "An overview on the light alcohol fuels in diesel engines." *Fuel* 236(2019): 890-911. https://doi.org/10.1016/j.fuel.2018.08.138.

[26] National Renewable Energy Laboratory. Co-Optimization of Fuels & Engines: Fuel Properties Database. Golden, Colorado: NREL. 2016.

[27] Koivisto, Elina, Nicos Ladommatos, and Martin Gold. "Compression Ignition and Exhaust Gas Emissions of Fuel Molecules Which Can Be Produced from Lignocellulosic Biomass: Levulinates, Valeric Esters, and Ketones." *Energy & Fuels* 29 9 (2015): 5875-5884. 10.1021/acs.energyfuels.5b01314.

[28] Mao, Gongping, and Sen Shao. "Experimental Research on the Flame Temperature of n-Butanol-Diesel Fuel Blends in Atmospheric Conditions." *Journal of Energy Engineering* 142 3 (2016): 04015037. doi:10.1061/(ASCE)EY.1943-7897.0000303.

[29] Davis, S. G., and C. K. Law. "Determination of and Fuel Structure Effects on Laminar Flame Speeds of C1 to C8 Hydrocarbons." *Combustion Science and Technology* 140 1-6 (1998): 427-449. 10.1080/00102209808915781.

[30] Zhang, Ni, Yage Di, Zuohua Huang, Bin Zheng, and Zhiyuan Zhang. "Experimental Study on Combustion Characteristics of N2-Diluted Diethyl Ether−Air Mixtures." *Energy & Fuels* 23 12 (2009): 5798-5805. 10.1021/ef900633z.

[31] Rakopoulos, D. C., C. D. Rakopoulos, R. G. Papagiannakis, and D. C. Kyritsis. "Combustion heat release analysis of ethanol or n-butanol diesel fuel blends in heavy-duty DI diesel engine." *Fuel* 90 5 (2011): 1855-1867. https://doi.org/10.1016/j.fuel.2010.12.003.

[32] Sayin, Cenk. "Engine performance and exhaust gas emissions of methanol and ethanol–diesel blends." *Fuel* 89 11 (2010): 3410-3415. https://doi.org/10.1016/j.fuel.2010.02.017.

[33] Heuser, Benedikt, Peter Mauermann, Rajendra Wankhade, Florian Kremer, and Stefan Pischinger. "Combustion and emission behavior of linear C8-oxygenates." *International Journal of Engine Research* 16 5 (2015): 627-638. 10.1177/1468087415594951.

[34] European Parliament. Regulation (EC) No 595/2009 of the European Parliament and of the Council of 18 June 2009 on type-approval of motor vehicles and engines with respect to emissions from heavy duty vehicles (Euro VI) and on access to vehicle repair and maintenance information and amending Regulation (EC)

No 715/2007 and Directive 2007/46/EC and repealing Directives 80/1269/EEC, 2005/55/EC and 2005/78/EC. 2009.
[35] European Commission. Proposal for a regulation of the European Parliament and of the Council on type-approval of motor vehicles and engines and of systems, components and separate technical units intended for such vehicles, with respect to their emissions and battery durability (Euro 7) and repealing Regulations (EC) No 715/2007 and (EC) No 595/2009. 2022.
[36] European Parliament, and European Council. REGULATION OF THE EUROPEAN PARLIAMENT AND OF THE COUNCIL on type-approval of motor vehicles and engines and of systems, components and separate technical units intended for such vehicles, with respect to their emissions and battery durability (Euro 7), amending Regulation (EU) 2018/858 of the European Parliament and of the Council and repealing Regulations (EC) No 715/2007 and (EC) No 595/2009 of the European Parliament and of the Council, Commission Regulation (EU) 582/2011, Commission Regulation (EU) 2017/1151, Commission Regulation (EU) 2017/2400 and Commission Implementing Regulation (EU) 2022/1362. 2024.
[37] European Parliament. Regulation (EU) 2016/1628 of the European Parliament And Of The Council of 14 September 2016 on requirements relating to gaseous and particulate pollutant emission limits and type-approval for internal combustion engines for non-road mobile machinery, amending Regulations (EU) No 1024/2012 and (EU) No 167/2013, and amending and repealing Directive 97/68/EC. 2016.
[38] *Reciprocating internal combustion engines. Exhaust emission measurement. Steady-state and transient test cycles for different engine applications.* BS ISO 8178-4:2020. Milton Keynes: BSI. 2020.
[39] Olanrewaju, Francis O., Hu Li, Gordon E. Andrews, and Herodotos N. Phylaktou. "Improved model for the analysis of the Heat Release Rate (HRR) in Compression Ignition (CI) engines." *Journal of the Energy Institute* 93 5 (2020): 1901-1913. https://doi.org/10.1016/j.joei.2020.04.005.
[40] Savitzky, Abraham, and M. J. E. Golay. "Smoothing and Differentiation of Data by Simplified Least Squares Procedures." *Analytical Chemistry* 36 8 (1964): 1627-1639. 10.1021/ac60214a047.
[41] Sher, Eran. *Handbook of air pollution from internal combustion engines: pollutant formation and control*.(Boston: Academic Press. 1998.)
[42] Reif, Konrad, and Karl-Heinz Dietsche. *Automotive handbook*. 9th edition, revised and extended / by Prof. Dr.-Ing. Konrad Reif, Dipl.-ing Karl-Heinz Dietsche ; and approx. 200 authors from industry and the university and college sector. ed. (Karlsruhe: Robert Bosch GmbH. 2014.)
[43] Robert Bosch Gmbh, ed. 2005. *Diesel-Engine Management*. Fourth edition completely revised and extended. ed. Plochingen: Robert Bosch Gmbh.
[44] Leach, FCP, MH Davy, and MS Peckham. "Cyclic NO2:NOx ratio from a diesel engine undergoing transient load steps." *International Journal of Engine Research* 22 1 (2021): 284-294. 10.1177/1468087419833202.
[45] Zhu, Haoyue, Stanislav V. Bohac, Kohei Nakashima, Luke M. Hagen, Zhen Huang, and Dennis N. Assanis. "Effect of fuel oxygen on the trade-offs between soot, NOx and combustion efficiency in premixed low-temperature diesel engine combustion." *Fuel* 112(2013): 459-465. https://doi.org/10.1016/j.fuel.2013.05.023.
[46] An, H., W. M. Yang, J. Li, and D. Z. Zhou. "Modeling study of oxygenated fuels on diesel combustion: Effects of oxygen concentration, cetane number and C/H ratio." *Energy Conversion and Management* 90(2015): 261-271. 10.1016/j.enconman.2014.11.031.
[47] Janssen, Andreas, Martin Muether, Stefan Pischinger, Andreas Kolbeck, and Matthias Lamping. 2009. "Tailor-Made Fuels: The Potential of Oxygen Content in Fuels for Advanced Diesel Combustion Systems." https://doi.org/10.4271/2009-01-2765.
[48] Jamrozik, Arkadiusz. "The effect of the alcohol content in the fuel mixture on the performance and emissions of a direct injection diesel engine fueled with diesel-methanol and diesel-ethanol blends." *Energy Conversion and Management* 148(2017): 461-476. https://doi.org/10.1016/j.enconman.2017.06.030.
[49] European Commission. Annexes to the Proposal for a regulation of the European Parliament and of the Council on type-approval of motor vehicles and engines and of systems, components and separate technical units intended for such vehicles, with respect to their emissions and battery durability (Euro 7) and repealing Regulations (EC) No 715/2007 and (EC) No 595/2009. 2022.
[50] Arias, Silvana, Maria L. Botero, Francisco Molina, and John R. Agudelo. "Pentanol/diesel fuel blends: Assessment of inhalation cancer risk and ozone formation potential from carbonyl emissions emitted by an automotive diesel engine." *Fuel* 321(2022): 124054. https://doi.org/10.1016/j.fuel.2022.124054.
[51] Atkinson, Roger. "Atmospheric chemistry of VOCs and NOx." *Atmospheric Environment* 34 12 (2000): 2063-2101. https://doi.org/10.1016/S1352-2310(99)00460-4.
[52] Goldmacher, Victor S., and William G. Thilly. "Formaldehyde is mutagenic for cultured human cells." *Mutation Research/Genetic Toxicology* 116 3 (1983): 417-422. https://doi.org/10.1016/0165-1218(83)90080-0.
[53] Anderson, L. G. "Effects of using renewable fuels on vehicle emissions." *Renewable & Sustainable Energy Reviews* 47(2015): 162-172. 10.1016/j.rser.2015.03.011.
[54] García, Antonio, José V. Pastor, Javier Monsalve-Serrano, and Erasmo Iñiguez. "Detailed assessment of exhaust emissions in a diesel engine running with low-carbon fuels via FTIR spectroscopy." *Fuel* 357(2024): 129707. https://doi.org/10.1016/j.fuel.2023.129707.
[55] Toumasatos, Zisimos, Hanwei Zhu, Thomas D. Durbin, Kent C. Johnson, Sam Cao, and Georgios Karavalakis. "Real-world particulate, GHG, and gaseous toxic emissions from heavy-duty diesel and natural gas vehicles." *Atmospheric Environment* 327(2024): 120512. https://doi.org/10.1016/j.atmosenv.2024.120512.
[56] Arias, Silvana, Francisco Molina, Rubén Palacio, Diana López, and John R. Agudelo. "Assessment of carbonyl and PAH emissions in an automotive diesel engine fueled with butanol and renewable diesel fuel blends." *Fuel* 316(2022): 123290. https://doi.org/10.1016/j.fuel.2022.123290.
[57] Sarathy, S. Mani, Patrick Oßwald, Nils Hansen, and Katharina Kohse-Höinghaus. "Alcohol combustion chemistry." *Progress in Energy and Combustion Science* 44(2014): 40-102. https://doi.org/10.1016/j.pecs.2014.04.003.
[58] Dempsey, Adam B, Scott J Curran, and Robert M Wagner. "A perspective on the range of gasoline compression ignition combustion strategies for high

engine efficiency and low NOx and soot emissions: Effects of in-cylinder fuel stratification." *International Journal of Engine Research* 17 8 (2016): 897-917. 10.1177/1468087415621805.

[59] Kitamura, T, T Ito, J Senda, and H Fujimoto. "Mechanism of smokeless diesel combustion with oxygenated fuels based on the dependence of the equivalence ration and temperature on soot particle formation." *International Journal of Engine Research* 3 4 (2002): 223-248. 10.1243/146808702762230923.

[60] Lao, Chung Ting, Jethro Akroyd, Nickolas Eaves, Alastair Smith, Neal Morgan, Daniel Nurkowski, Amit Bhave, and Markus Kraft. "Investigation of the impact of the configuration of exhaust after-treatment system for diesel engines." *Applied Energy* 267(2020): 114844. https://doi.org/10.1016/j.apenergy.2020.114844.

Appendices

A1.1 Ignition Delay

Table A1.1.1. Ignition delay in CAD for each butyl-based blend at the five engine loads tested. The uncertainty is 0.5 CAD, as this is the error in the accuracy of the timing of the pressure transducer, which is larger than the standard deviations.

Fuel	4% Load (CAD)	28% Load (CAD)	50% Load (CAD)	75% Load (CAD)	92% Load (CAD)
D100	22.0	21.6	21.3	21.2	21.6
D90Bu10 – 65:30:5	22.7	22.0	22.3	21.9	22.1
D90Bu10 – 75:20:5	22.9	22.7	22.4	22.3	22.6
D90Bu10 – 85:10:5	23.1	22.7	22.5	22.2	22.4
D90Bu10 – 85:5:10	23.3	22.5	22.0	21.9	22.3
D90Bu10 – 90:5:5	23.3	22.5	22.0	21.9	22.0
D75Bu25 – 85:10:5	24.1	24.1	23.3	23.1	23.4
D75Bu25 – 90:5:5	24.5	24.0	23.6	23.5	23.6

Table A1.1.2. Ignition delay in ms for each butyl-based blend at the five engine loads tested. The uncertainty is 0.3 ms as this is equivalent to 0.5 CAD, which is the error in the accuracy of the timing of the pressure transducer, which is larger than the standard deviations.

Fuel	4% Load (ms)	28% Load (ms)	50% Load (ms)	75% Load (ms)	92% Load (ms)
D100	1.17	1.16	1.15	1.15	1.18
D90Bu10 – 65:30:5	1.21	1.19	1.20	1.19	1.21
D90Bu10 – 75:20:5	1.22	1.22	1.21	1.21	1.24
D90Bu10 – 85:10:5	1.23	1.22	1.22	1.20	1.23
D90Bu10 – 85:5:10	1.24	1.21	1.19	1.19	1.22
D90Bu10 – 90:5:5	1.24	1.21	1.19	1.19	1.21
D75Bu25 – 85:10:5	1.28	1.30	1.26	1.26	1.28
D75Bu25 – 90:5:5	1.32	1.29	1.28	1.28	1.30

Table A1.1.3. Changes in IDT for each butyl-based blend relative to diesel (D100) at the five engine loads tested. The uncertainties were determined using error propagation of the diesel and biofuel blends.

Fuel	Relative Change at 4% Load (%)	Relative Change at 28% Load (%)	Relative Change at 50% Load (%)	Relative Change at 75% Load (%)	Relative Change at 92% Load (%)
D90Bu10 – 65:30:5	3.59 ± 3.28	2.20 ± 3.31	4.83 ± 4.09	3.47 ± 3.40	2.24 ± 3.31
D90Bu10 – 75:20:5	4.28 ± 2.37	5.09 ± 3.36	5.43 ± 3.41	5.24 ± 3.43	4.86 ± 3.36
D90Bu10 – 85:10:5	5.06 ± 3.30	5.35 ± 3.36	5.89 ± 3.42	4.68 ± 3.42	3.85 ± 3.34
D90Bu10 – 85:5:10	6.19 ± 3.32	4.66 ± 3.36	3.53 ± 3.38	3.77 ± 3.41	3.28 ± 3.33
D90Bu10 – 90:5:5	5.72 ± 3.31	4.33 ± 3.35	3.56 ± 2.35	3.51 ± 3.40	2.10 ± 3.31
D75Bu25 – 85:10:5	9.61 ± 3.38	11.72 ± 3.47	9.68 ± 3.49	9.51 ± 3.51	8.36 ± 3.42
D75Bu25 – 90:5:5	12.29 ± 3.43	11.44 ± 3.47	11.18 ± 2.61	11.23 ± 3.54	10.03 ± 3.45

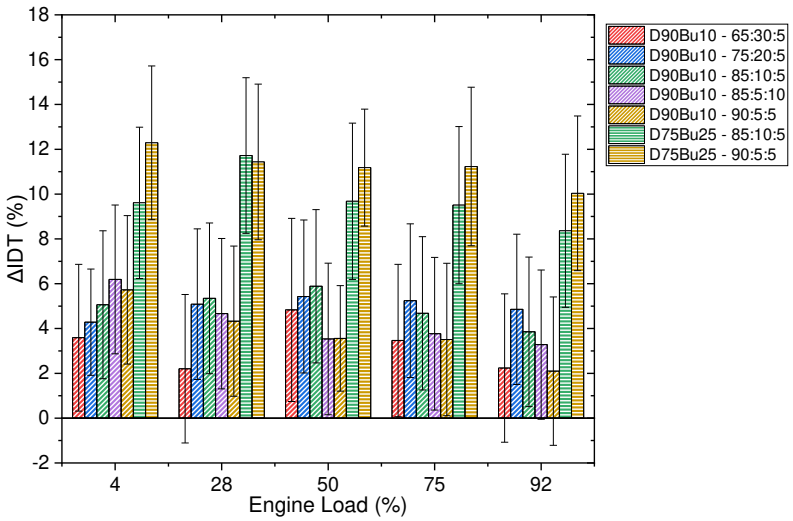

Figure A1.1.1. Relative percentage changes in the IDT in milliseconds relative to D100.

A1.2 In-cylinder Peak Pressure

Table A1.2.1. In-cylinder pressure for each butyl-based blend at the five engine loads tested. The uncertainties are the standard deviations from the three repeats.

Fuel	4% Load (bar)	28% Load (bar)	50% Load (bar)	75% Load (bar)	92% Load (bar)
D100	59.1 ± 0.2	62.7 ± 0.4	64.4 ± 1.0	66.6 ± 0.4	69.3 ± 0.7
D90Bu10 – 65:30:5	57.7 ± 0.9	61.6 ± 0.2	64.4 ± 0.3	66.1 ± 0.3	68.6 ± 0.2
D90Bu10 – 75:20:5	58.7 ± 0.3	61.9 ± 0.2	64.7 ± 0.5	66.8 ± 0.6	69.3 ± 0.2
D90Bu10 – 85:10:5	58.5 ± 0.5	62.1 ± 0.4	64.6 ± 0.1	66.9 ± 0.1	69.7 ± 0.01
D90Bu10 – 85:5:10	55.6 ± 0.5	60.1 ± 0.5	62.5 ± 0.5	65.1 ± 0.7	67.5 ± 0.5
D90Bu10 – 90:5:5	55.7 ± 0.3	60.3 ± 0.5	62.8 ± 0.9	64.9 ± 0.7	67.2 ± 0.2
D75Bu25 – 85:10:5	56.1 ± 0.4	59.9 ± 0.2	62.7 ± 0.1	65.9 ± 0.6	69.0 ± 0.3
D75Bu25 – 90:5:5	56.6 ± 0.6	60.2 ± 1.1	64.5 ± 0.1	65.8 ± 0.8	69.5 ± 1.1

Table A1.2.2. Changes in in-cylinder pressure for each butyl-based blend relative to diesel (D100) at the five engine loads tested. The uncertainties were determined using error propagation of the standard deviations of the diesel and biofuel blends.

Fuel	Relative Change at 4% Load (%)	Relative Change at 28% Load (%)	Relative Change at 50% Load (%)	Relative Change at 75% Load (%)	Relative Change at 92% Load (%)
D90Bu10 – 65:30:5	-2.29 ± 1.28	-1.77 ± 0.84	0.01 ± 1.73	-0.79 ± 0.90	-1.08 ± 1.15
D90Bu10 – 75:20:5	-0.64 ± 0.80	-1.37 ± 0.87	0.41 ± 1.82	0.25 ± 1.19	-0.05 ± 1.17
D90Bu10 – 85:10:5	-0.95 ± 0.96	-0.99 ± 1.05	0.23 ± 1.63	0.47 ± 0.72	0.61 ± 1.04
D90Bu10 – 85:5:10	-5.91 ± 1.02	-4.21 ± 1.08	-2.89 ± 1.76	-2.26 ± 1.18	-2.58 ± 1.30
D90Bu10 – 90:5:5	-5.76 ± 0.78	-3.91 ± 1.09	-2.57 ± 1.94	-2.59 ± 1.19	-3.00 ± 1.10
D75Bu25 – 85:10:5	-5.09 ± 0.94	-4.56 ± 0.80	-2.67 ± 1.57	-1.03 ± 1.13	-0.45 ± 1.23
D75Bu25 – 90:5:5	-4.00 ± 0.94	-4.13 ± 1.49	0.07 ± 1.64	-1.15 ± 1.30	0.34 ± 1.63

A1.3 Brake Specific Fuel Consumption

Table A1.3.1. BSFC for each butyl-based blend at the five engine loads tested. The uncertainties are the standard deviations from the three repeats.

Fuel	4% Load (g/kWh)	28% Load (g/kWh)	50% Load (g/kWh)	75% Load (g/kWh)	92% Load (g/kWh)
D100	1945 ± 8.01	395 ± 18.1	292 ± 6.39	260 ± 4.26	272 ± 3.44
D90Bu10 – 65:30:5	2003 ± 42.3	396 ± 46.7	294 ± 7.00	267 ± 6.84	270 ± 5.08
D90Bu10 – 75:20:5	1995 ± 51.2	414 ± 0.37	293 ± 4.81	269 ± 10.8	271 ± 3.71
D90Bu10 – 85:10:5	1967 ± 89.3	414 ± 0.33	301 ± 0.11	259 ± 5.52	273 ± 3.53
D90Bu10 – 85:5:10	1974 ± 2.08	404 ± 16.4	300 ± 6.18	268 ± 2.99	278 3.80
D90Bu10 – 90:5:5	2054 ± 68.1	420 ± 4.52	298 ± 6.83	266 ± 1.18	275 ± 0.75
D75Bu25 – 85:10:5	2160 ± 66.2	440 ± 11.6	319 ± 12.0	280 ± 4.42	293 ± 3.73
D75Bu25 – 90:5:5	2286 ± 60.8	455 ± 14.9	314 ± 7.99	290 ± 1.01	302 ± 5.50

Table A1.3.2. Changes in BSFC for each butyl-based blend relative to diesel (D100) at the five engine loads tested. The uncertainties were determined using error propagation of the standard deviations of the diesel and biofuel blends.

Fuel	Relative Change at 4% Load (%)	Relative Change at 28% Load (%)	Relative Change at 50% Load (%)	Relative Change at 75% Load (%)	Relative Change at 92% Load (%)
D90Bu10 – 65:30:5	3.00 ± 2.22	0.41 ± 12.7	0.58 ± 3.25	2.53 ± 3.12	-0.97 ± 2.24
D90Bu10 – 75:20:5	2.57 ± 2.67	4.83 ± 4.82	0.36 ± 2.74	3.46 ± 4.49	-0.38 ± 1.85
D90Bu10 – 85:10:5	1.17 ± 4.61	4.77 ± 4.81	2.86 ± 2.25	-0.27 ± 2.77	0.33 ± 1.81
D90Bu10 – 85:5:10	1.50 ± 0.43	2.32 ± 6.27	2.55 ± 3.08	2.85 ± 2.04	1.97 ± 1.90
D90Bu10 – 90:5:5	5.60 ± 3.53	6.51 ± 5.02	1.82 ± 3.23	2.30 ± 1.74	1.09 ± 1.30
D75Bu25 – 85:10:5	11.08 ± 3.43	11.37 ± 5.90	9.25 ± 4.76	7.73 ± 2.45	7.60 ± 1.93
D75Bu25 – 90:5:5	17.53 ± 2015	15.35 ± 6.51	7.40 ± 3.60	11.66 ± 1.87	10.27 ± 2.45

A1.4 Heat Release Rates

Table A1.4.1. Peak heat release rates (HRRs) for each butyl-based blend at the selected engine loads.

Fuel	50% Load (J/CAD)	92% Load (J/CAD)
D100	36.58	38.95
D90Bu10 – 65:30:5	34.99	39.82
D90Bu10 – 85:10:5	35.82	45.38
D90Bu10 – 90:5:5	32.66	41.80
D75Bu25 – 85:10:5	35.52	45.18
D75Bu25 – 90:5:5	38.69	49.20

Table S1.4.2. Changes in peak HRR for each butyl-based blend relative to diesel (D100) at the selected engine loads.

Fuel	Relative Change at 50% Load (%)	Relative Change at 92% Load (%)
D90Bu10 – 65:30:5	-4.36	2.24
D90Bu10 – 85:10:5	-2.08	16.52
D90Bu10 – 90:5:5	-10.7	7.32
D75Bu25 – 85:10:5	-2.90	16.0
D75Bu25 – 90:5:5	5.77	26.3

Table S1.4.3. Timing of peak HRR and change in timing for each butyl-based blend at the selected engine loads. The uncertainties are 0.5 CAD, the uncertainty in the pressure transducer timing.

Fuel	50% Load (CAD)	Change in Timing at 50% Load (CAD)	92% Load (CAD)	Change in Timing at 92% Load (CAD)
D100	7.5		8.5	
D90Bu10 – 65:30:5	9.0	1.5	9.0	0.5
D90Bu10 – 85:10:5	9.5	2.0	9.5	1.0
D90Bu10 – 90:5:5	9.0	1.5	9	0.5
D75Bu25 – 85:10:5	10.5	3.0	10.5	2.0
D75Bu25 – 90:5:5	11.5	4.0	10.5	2.0

A2 Gaseous Emissions Data

A2.1 CO Emissions Data

Table A2.1.1. Specific CO emissions for each biofuel blend at the five engine loads tested. The uncertainties are the standard deviations from the three repeats.

Fuel	4% Load (g/kWh)	28% Load (g/kWh)	50% Load (g/kWh)	75% Load (g/kWh)	92% Load (g/kWh)
D100	61.8 ± 1.1	9.6 ± 0.6	5.0 ± 0.3	2.8 ± 0.1	2.2 ± 0.1
D90Bu10 – 65:30:5	76.3 ± 10.6	10.3 ± 1.0	6.4 ± 0.04	3.1 ± 0.2	2.0 ± 0.03
D90Bu10 – 75:20:5	79.5 ± 3.3	11.5 ± 0.6	6.3 ± 0.3	3.6 ± 0.1	2.2 ± 0.1
D90Bu10 – 85:10:5	88.1 ± 1.2	13.4 ± 0.9	6.8 ± 0.1	3.3 ± 0.1	2.4 ± 0.2
D90Bu10 – 85:5:10	90.3 ± 3.3	13.0 ± 0.6	6.5 ± 0.3	3.4 ± 0.1	2.4 ± 0.1
D90Bu10 – 90:5:5	92.3 1.2	13.5 ± 0.2	6.6 ± 0.1	3.3 ± 0.1	2.3 ± 0.1
D75Bu25 – 85:10:5	124.4 ± 8.1	17.8 ± 0.4	8.2 ± 0.5	4.1 ± 0.1	2.6 ± 0.04
D75Bu25 – 90:5:5	134.8 ± 6.2	19.2 ± 0.7	9.5 ± 0.4	4.8 ± 0.1	2.9 ± 0.3

Table A2.1.2. Changes in CO emissions for each biofuel blend relative to diesel (D100) at the five engine loads tested. The uncertainties were determined using error propagation of the standard deviations of the diesel and biofuel blends.

Fuel	Relative Change at 4% Load (%)	Relative Change at 28% Load (%)	Relative Change at 50% Load (%)	Relative Change at 75% Load (%)	Relative Change at 92% Load (%)
D90Bu10 – 65:30:5	23.6 ± 17.3	7.0 ± 12.5	28.0 ± 8.2	10.7 ± 5.7	-8.1 ± 3.0
D90Bu10 – 75:20:5	28.7 ± 5.7	19.0 ± 9.7	27.0 ± 9.7	26.2 ± 5.1	-0.4 ± 7.5
D90Bu10 – 85:10:5	42.6 ± 3.2	38.6 ± 12.8	36.2 ± 9.1	18.4 ± 3.8	9.1 ± 7.7
D90Bu10 – 85:5:10	46.2 ± 5.9	34.3 ± 10.2	29.8 ± 9.9	20.7 ± 5.2	9.8 ± 5.5
D90Bu10 – 90:5:5	49.4 ± 3.3	39.7 ± 9.1	31.2 ± 8.5	17.1 ± 3.0	6.4 ± 4.6
D75Bu25 – 85:10:5	101.4 ± 13.6	84.8 ± 12.4	63.2 ± 13.8	44.3 ± 3.3	22.0 ± 3.9
D75Bu25 – 90:5:5	118.2 ± 10.7	99.4 ± 14.4	90.0 ± 14.8	71.3 ± 4.7	34.1 ± 12.6

A2.2 Total Hydrocarbon Emissions Data

Table A2.2.1. Specific total hydrocarbon emissions for each biofuel blend at the five engine loads tested. The uncertainties are the standard deviations from the three repeats.

Fuel	4% Load (g/kWh)	28% Load (g/kWh)	50% Load (g/kWh)	75% Load (g/kWh)	92% Load (g/kWh)
D100	25.4 ± 2.9	3.93 ± 0.31	1.80 ± 0.11	0.86 ± 0.07	0.81 ± 0.06
D90Bu10 – 65:30:5	28.8 ± 4.9	3.87 ± 0.31	2.05 ± 0.16	0.89 ± 0.12	0.58 ± 0.07
D90Bu10 – 75:20:5	29.7 ± 0.6	4.21 ± 0.32	2.19 ± 0.03	1.15 ± 0.18	0.75 ± 0.12
D90Bu10 – 85:10:5	34.5 ± 2.5	4.64 ± 0.13	2.19 ± 0.01	0.92 ± 0.04	0.82 ± 0.06
D90Bu10 – 85:5:10	41.5 ± 6.2	4.52 ± 0.19	2.21 ± 0.15	0.92 ± 0.09	0.81 ± 0.08
D90Bu10 – 90:5:5	40.6 ± 2.8	4.52 ± 0.21	2.15 ± 0.13	0.83 ± 0.08	0.75 ± 0.06
D75Bu25 – 85:10:5	46.13 ± 4.0	5.90 ± 0.17	2.44 ± 0.14	1.01 ± 0.07	0.84 ± 0.07
D75Bu25 – 90:5:5	43.3 ± 3.3	4.80 ± 0.14	2.34 ± 0.01	0.93 ± 0.8	0.68 ± 0.02

Table A2.2.2. Changes in total hydrocarbon emissions for each biofuel blend relative to diesel (D100) at the five engine loads tested. The uncertainties were determined using error propagation of the standard deviations of the diesel and biofuel blends.

Fuel	Relative Change at 4% Load (%)	Relative Change at 28% Load (%)	Relative Change at 50% Load (%)	Relative Change at 75% Load (%)	Relative Change at 92% Load (%)
D90Bu10 – 65:30:5	13.3 ± 23.3	-1.4 ± 11.1	13.9 ± 11.3	2.6 ± 16.3	-28.3 ± 10.5
D90Bu10 – 75:20:5	16.7 ± 13.5	7.1 ± 11.8	21.6 ± 7.7	33.0 ± 23.5	-7.0 ± 16.8
D90Bu10 – 85:10:5	35.7 ± 18.3	18.1 ± 9.9	21.6 ± 7.6	6.3 ± 9.9	1.2 ± 10.9
D90Bu10 – 85:5:10	63.2 ± 30.6	15.1 ± 10.4	22.6 ± 11.4	6.6 ± 13.8	-0.5 ± 12.4
D90Bu10 – 90:5:5	59.7 ± 21.3	15.0 ± 10.6	19.1 ± 10.5	-4.6 ± 12.2	-7.5 ± 10.4
D75Bu25 – 85:10:5	81.5 ± 25.9	50.2 ± 12.7	35.5 ± 12.5	16.3 ± 12.4	3.9 ± 12.0
D75Bu25 – 90:5:5	70.5 ± 23.3	22.1 ± 10.4	29.4 ± 8.0	7.3 ± 12.6	-15.5 ± 7.1

A2.3 Nitrogen Oxides (NO_X) Emissions Data

Table A2.3.1. Specific nitrogen oxides (NOx) emissions for each biofuel blend at the five engine loads tested. The uncertainties are the standard deviations from the three repeats.

Fuel	4% Load (g/kWh)	28% Load (g/kWh)	50% Load (g/kWh)	75% Load (g/kWh)	92% Load (g/kWh)
D100	31.6 ± 0.6	7.3 ± 0.4	5.5 ± 0.05	5.3 ± 0.1	5.9 ± 0.8
D90Bu10 – 65:30:5	28.9 ± 2.6	6.6 ± 0.7	5.4 ± 0.3	4.9 ± 0.3	5.3 ± 0.2
D90Bu10 – 75:20:5	29.6 ± 1.7	6.9 ± 0.5	5.4 ± 0.4	5.3 ± 0.5	5.6 ± 0.2
D90Bu10 – 85:10:5	31.0 ± 1.8	7.4 ± 0.2	5.8 ± 0.1	5.4 ± 0.04	6.1 ± 0.04
D90Bu10 – 85:5:10	28.6 ± 0.2	7.2 ± 0.4	5.7 ± 0.2	5.6 ± 0.1	6.2 ± 0.3
D90Bu10 – 90:5:5	31.7 ± 1.5	7.8 ± 0.2	5.8 ± 0.3	5.7 ± 0.1	6.4 ± 0.1
D75Bu25 – 85:10:5	28.1 ± 0.5	7.0 ± 0.3	5.6 ± 0.2	5.4 ± 0.1	6.3 ± 0.1
D75Bu25 – 90:5:5	31.5 ± 0.7	7.5 ± 0.2	5.8 ± 0.3	5.5 ± 0.1	6.8 ± 0.2

Table A2.3.2. Changes in nitrogen oxides (NOx) emissions for each biofuel blend relative to diesel (D100) at the five engine loads tested. The uncertainties were determined using error propagation of the standard deviations of the diesel and biofuel blends.

Fuel	Relative Change at 4% Load (%)	Relative Change at 28% Load (%)	Relative Change at 50% Load (%)	Relative Change at 75% Load (%)	Relative Change at 92% Load (%)
D90Bu10 – 65:30:5	-8.6 ± 8.5	-9.2 ± 10.3	-2.0 ± 6.1	-6.7 ± 5.5	-9.7 ± 3.9
D90Bu10 – 75:20:5	-6.3 ± 5.8	-4.6 ± 8.2	-2.0 ± 6.9	-0.8 ± 10.0	-5.1 ± 3.8
D90Bu10 – 85:10:5	-1.9 ± 6.0	1.6 ± 6.0	5.8 ± 2.6	2.6 ± 2.8	4.6 ± 1.6
D90Bu10 – 85:5:10	-9.3 ± 1.9	-1.3 ± 7.9	2.6 ± 3.1	5.2 ± 3.4	5.2 ± 4.8
D90Bu10 – 90:5:5	0.3 ± 5.1	6.9 ± 6.3	5.7 ± 5.1	6.9 ± 3.6	8.1 ± 2.0
D75Bu25 – 85:10:5	-11.1 ± 2.4	-3.5 ± 6.1	0.6 ± 3.6	1.3 ± 2.8	6.9 ± 1.8
D75Bu25 – 90:5:5	-0.1 ± 3.8	2.5 ± 3.8	4.8 ± 5.6	3.4 ± 5.9	16.1 ± 2.9

A2.4 Aldehyde Emissions Data

Table A2.4.1. Average formaldehyde concentrations for each biofuel blend at the five engine loads tested. The uncertainties are the standard deviations from the three repeats.

Fuel	4% Load (ppm)	28% Load (ppm)	50% Load (ppm)	75% Load (ppm)	92% Load (ppm)
D100	13.75 ± 0.81	12.43 ± 0.81	8.68 ± 1.82	4.84 ± 0.52	4.81 ± 0.98
D90Bu10 – 65:30:5	20.55 ± 3.47	14.19 ± 0.75	14.48 ± 1.54	7.18 ± 1.08	4.15 ± 0.17
D90Bu10 – 75:20:5	22.37 ± 2.85	15.82 ± 1.87	13.16 ± 0.69	7.73 ± 1.49	5.00 ± 0.66
D90Bu10 – 85:10:5	26.08 ± 0.90	19.73 ± 2.17	14.16 ± 0.36	7.74 ± 0.52	4.46 ± 0.44
D90Bu10 – 85:5:10	29.58 ± 2.64	19.06 ±1.05	13.46 ± 0.97	7.70 ± 1.22	5.91 ± 0.61
D90Bu10 – 90:5:5	28.71 ± 1.89	18.43 ± 0.91	13.39 ± 0.30	6.67 ± 0.15	5.40 ± 0.73
D75Bu25 – 85:10:5	39.48 ± 1.86	28.11 ± 0.67	17.90 ± 0.73	9.08 ± 0.47	5.49 ± 0.32
D75Bu25 – 90:5:5	35.83 ± 2.05	24.61 ± 0.32	18.32 ± 0.84	9.81 ± 0.50	5.79 ± 0.72

Table A2.4.2. Average acetaldehyde concentrations for each biofuel blend at the five engine loads tested. The uncertainties are the standard deviations from the three repeats.

Fuel	4% Load (ppm)	28% Load (ppm)	50% Load (ppm)	75% Load (ppm)	92% Load (ppm)
D100	5.62 ± 1.05	4.25 ± 0.64	5.21 ± 1.68	5.98 ± 2.09	6.80 ± 1.04
D90Bu10 – 65:30:5	8.46 ± 1.83	5.18 ± 1.55	5.43± 1.86	5.00 ± 0.68	6.06 ± 1.76
D90Bu10 – 75:20:5	8.71 ± 0.68	5.93 ± 1.00	7.88 ± 0.22	5.99 ± 1.73	7.78 ± 0.70
D90Bu10 – 85:10:5	11.11 ± 0.34	8.17 ± 0.88	5.00 ± 2.11	5.13 ± 1.45	6.95 ± 1.98
D90Bu10 – 85:5:10	11.43 ± 0.75	6.46 ± 1.11	4.25 ± 0.36	4.23 ± 0.60	5.34 ± 0.64
D90Bu10 – 90:5:5	11.34 ± 0.90	6.96 ± 1.63	5.14 ± 1.95	3.99 ± 1.61	4.70 ± 1.38
D75Bu25 – 85:10:5	13.92 ± 0.10	9.33 ± 0.44	6.22 ± 0.68	4.90 ± 0.85	6.02 ± 0.20
D75Bu25 – 90:5:5	10.35 ± 0.19	6.71 ± 0.43	6.14 ± 0.30	4.84 ± 1.39	6.11 ± 1.38

A3 Particulate Matter Emissions Data

A3.1 $PM_{2.5}$ Data

Table A3.1.1. Specific $PM_{2.5}$ emissions for each biofuel blend at the five engine loads tested. The uncertainties are the standard deviations from the three repeats.

Fuel	4% Load (g/kWh)	28% Load (g/kWh)	50% Load (g/kWh)	75% Load (g/kWh)	92% Load (g/kWh)
D100	7.99 ± 0.33	0.25 ± 0.05	0.09 ± 0.01	0.051 ± 0.001	0.055 ± 0.005
D90Bu10 – 65:30:5	5.08 ± 1.18	0.189 ± 0.04	0.065 ± 0.01	0.041 ± 0.004	0.043 ± 0.01
D90Bu10 – 75:20:5	4.55 ± 0.64	0.15 ± 0.01	0.065 ± 0.02	0.04 ± 0.01	0.04 ± 0.01
D90Bu10 – 85:10:5	4.58 ± 0.62	0.15 ± 0.03	0.06 ± 0.01	0.029 ± 0.002	0.0541 ± 0.0003
D90Bu10 – 85:5:10	3.71 ± 0.86	0.13 ± 0.02	0.05 ± 0.01	0.03 ± 0.01	0.04 ± 0.01
D90Bu10 – 90:5:5	3.98 ± 1.26	0.14 ± 0.04	0.05 ± 0.02	0.03 ± 0.01	0.04 0.01
D75Bu25 – 85:10:5	2.37 ± 0.62	0.12 ± 0.03	0.044 ± 0.01	0.0214 ± 0.0004	0.032 ± 0.003
D75Bu25 – 90:5:5	2.88 ± 0.047	0.11 ± 0.01	0.06 ± 0.01	0.021 ± 0.001	0.03 ± 0.01

Table A3.1.2. Changes in $PM_{2.5}$ emissions for each biofuel blend relative to diesel (D100) at the five engine loads tested. The uncertainties were determined using error propagation of the standard deviations of the diesel and biofuel blends.

Fuel	Relative Change at 4% Load (%)	Relative Change at 28% Load (%)	Relative Change at 50% Load (%)	Relative Change at 75% Load (%)	Relative Change at 92% Load (%)
D90Bu10 – 65:30:5	-36.4 ± 15.1	-24.2 ± 17.5	-27.0 ± 15.8	-19.8 ± 8.6	-21.8 ± 13.6
D90Bu10 – 75:20:5	-43.0 ± 8.4	-41.4 ± 11.4	-26.9 ± 19.1	-26.0 ± 25.2	-19.2 ± 13.4
D90Bu10 – 85:10:5	-42.7 ± 8.2	-38.8 ± 16.8	-36.5 ± 7.6	-43.3 ± 3.4	-1.0 ± 6.7
D90Bu10 – 85:5:10	-53.6 ± 10.9	-49.0 ± 11.1	-49.6 ± 8.2	-45.0 ± 11.4	-22.4 ± 26.6
D90Bu10 – 90:5:5	-50.2 ± 15.9	-43.3 ± 18.1	-44.9 ± 15.4	-39.2 ± 21.7	-25.3 ± 15.5
D75Bu25 – 85:10:5	-70.4 ± 5.8	-53.4 ± 14.5	-50.4 ± 11.1	-58.0 ± 1.4	-40.3 ± 7.4
D75Bu25 – 90:5:5	-64.0 ± 6.1	-55.3 ± 9.0	-34.1 ± 10.1	-59.7 ± 1.8	-40.2 ± 20.7

A3.2 Particle Number Data

Table A3.2.1. Specific particle number (PN) emissions for each biofuel blend at the five engine loads tested. The uncertainties are the standard deviations from the three repeats.

Fuel	4% Load ((#/cc)/kWh) $\times 10^8$	28% Load ((#/cc)/kWh) $\times 10^8$	50% Load ((#/cc)/kWh) $\times 10^8$	75% Load ((#/cc)/kWh) $\times 10^8$	92% Load ((#/cc)/kWh) $\times 10^8$
D100	12.9 ± 0.2	2.27 ± 0.08	1.79 ± 0.03	1.54 ± 0.06	1.32 ± 0.01
D90Bu10 – 65:30:5	3.18 ± 0.36	0.67 ± 0.04	0.42 ± 0.05	0.47 ± 0.01	0.454 ± 0.003
D90Bu10 – 75:20:5	2.98 ± 0.46	0.62 ± 0.08	0.417 ± 0.003	0.42 ± 0.01	0.48 ± 0.01
D90Bu10 – 85:10:5	2.89 ± 0.21	0.62 ± 0.05	0.43 ± 0.03	0.37 ± 0.08	0.45 ± 0.03
D90Bu10 – 85:5:10	2.75 ± 0.16	0.56 ± 0.06	0.38 ± 0.01	0.373 ± 0.004	0.44 ± 0.03
D90Bu10 – 90:5:5	2.67 ± 0.10	0.59 ± 0.08	0.39 ± 0.01	0.38 ± 0.01	0.43 ± 0.01
D75Bu25 – 85:10:5	1.57 ± 0.12	0.35 ± 0.05	0.30 ± 0.02	0.29 ± 0.02	0.35 ± 0.01
D75Bu25 – 90:5:5	4.72 ± 0.23	1.03 ± 0.16	0.78 ± 0.10	0.72 ± 0.03	0.82 ± 0.04

Table A3.2.2. Changes in PN emissions for each biofuel blend relative to diesel (D100) at the five engine loads tested. The uncertainties were determined using error propagation of the standard deviations of the diesel and biofuel blends.

Fuel	Relative Change at 4% Load (%)	Relative Change at 28% Load (%)	Relative Change at 50% Load (%)	Relative Change at 75% Load (%)	Relative Change at 92% Load (%)
D90Bu10 – 65:30:5	-75.4 ± 2.8	-70.7 ± 1.9	-76.7 ± 2.9	-69.3 ± 1.3	-65.6 ± 0.3
D90Bu10 – 75:20:5	-77.0 ± 3.5	-72.8 ± 3.7	-76.7 ± 0.4	-73.0 ± 1.1	-63.8 ± 0.6
D90Bu10 – 85:10:5	-77.7 ± 1.6	-72.9 ± 2.6	-76.0 ± 1.9	-76.2 ± 5.3	-66.2 ± 2.5
D90Bu10 – 85:5:10	-78.8 ± 1.3	-75.4 ± 2.7	-78.5 ± 0.4	-75.8 ± 0.9	-66.5 ± 1.9
D90Bu10 – 90:5:5	-79.3 ± 0.8	-74.1 ± 3.5	-78.1 ± 0.5	-75.0 ± 1.2	-67.3 ± 1.1
D75Bu25 – 85:10:5	-87.9 ± 1.0	-84.7 ± 2.1	-83.5 ± 1.0	-81.1 ± 1.4	-73.6 ± 0.6
D75Bu25 – 90:5:5	-63.5 ± 1.9	-54.9 ± 7.1	-56.5 ± 5.4	-53.0 ± 2.4	-37.8 ± 3.2

A3.3 Particle Number Size Distributions

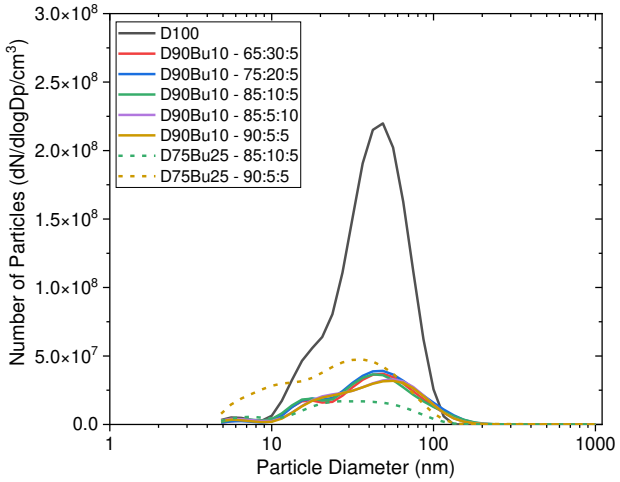

Figure A3.1. Particle number size distributions for the butyl-based blends at 4% load.

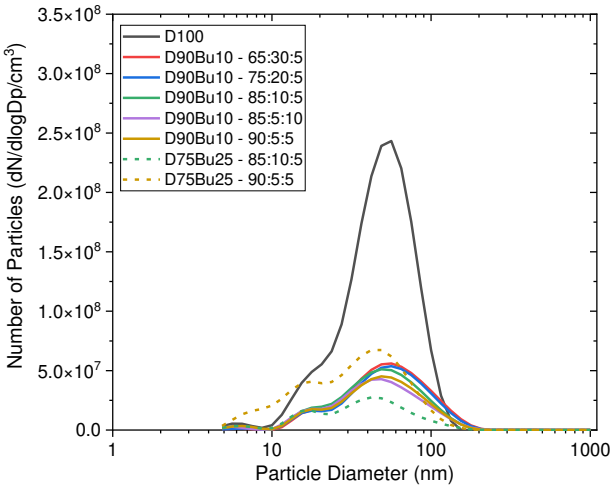

Figure A3.2. Particle number size distributions for the butyl-based blends at 28% load.

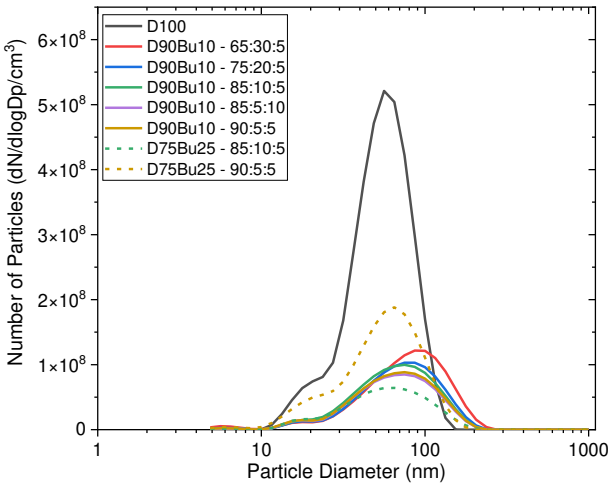

Figure A3.3. Particle number size distributions for the butyl-based blends at 75% load.